NASA TECHNICAL NOTE NASA TN D-3966

NASA TN D-3966

THE INFLUENCE OF RESPONSE FEEDBACK LOOPS ON THE LATERAL-DIRECTIONAL DYNAMICS OF A VARIABLE-STABILITY TRANSPORT AIRCRAFT

by Kenneth J. Szalai

Flight Research Center
Edwards, Calif.

NATIONAL AERONAUTICS AND SPACE ADMINISTRATION • WASHINGTON, D. C. • MAY 1967

NASA TN D-3966

THE INFLUENCE OF RESPONSE FEEDBACK LOOPS ON THE LATERAL-DIRECTIONAL DYNAMICS OF A VARIABLE-STABILITY TRANSPORT AIRCRAFT

By Kenneth J. Szalai

Flight Research Center
Edwards, Calif.

NATIONAL AERONAUTICS AND SPACE ADMINISTRATION

For sale by the Clearinghouse for Federal Scientific and Technical Information
Springfield, Virginia 22151 – CFSTI price $3.00

THE INFLUENCE OF RESPONSE FEEDBACK LOOPS ON THE LATERAL-DIRECTIONAL DYNAMICS OF A VARIABLE-STABILITY TRANSPORT AIRCRAFT

By Kenneth J. Szalai
Flight Research Center

SUMMARY

Several response feedback loops are analyzed to determine their effects on the lateral-directional dynamics of a variable-stability transport aircraft. The response feedback system feeds back response variables such as sideslip angle or roll rate as rudder or aileron commands, or both, thus altering the various transfer functions which describe the dynamic characteristics of the aircraft. The range of feedback gain for which approximate expressions are valid in describing the effect of a particular loop is noted. The root-locus method is used to show how the Dutch roll, roll, and spiral modes are influenced as a function of feedback gain. Expressions are developed which directly relate feedback gains to some response parameter, such as Dutch roll frequency, damping ratio, or roll and spiral mode time constants. The expansion to multiloop systems is discussed, along with limitations of the response feedback system, from the standpoint of operating a variable-stability aircraft.

INTRODUCTION

In conjunction with the design and development of a general purpose airborne simulator[1] (GPAS), studies were made at the NASA Flight Research Center of response feedback control loops and their influence on the GPAS, a variable-stability Lockheed JetStar aircraft. Although much information has been published on variable-stability aircraft, no single document contains a development of the fundamental concepts of response feedback systems along with a detailed discussion of loops that are utilized in variable-stability aircraft. Reference 1 is concerned primarily with showing the feasibility of installing a response feedback system (RFS) in a T-33 aircraft. The theoretical treatment is limited to showing that the aerodynamic coefficients of the equations of motion of the T-33 can be altered to match the coefficients of an aircraft to be simulated. The report does not analyze specific loops in detail, nor does it predict how individual loops influence the dynamic modes of the aircraft. It is not an adequate source of basic information on analysis techniques. Reference 2 is typical of many reports which emphasize research results of using an RFS aircraft but do not present

---

[1]NASA Contract NAS4-607 with the Cornell Aeronautical Laboratory, Inc., Buffalo, N. Y..

much background material on the theoretical basis of the system. This particular reference does contain several approximations derived from the equations of motion which are useful in describing the effects of certain RFS loops.

A qualitative description of a response feedback system is given in reference 3, which discusses airborne simulation in general and its applications in research and training. Reference 4 is devoted entirely to one loop configuration and its effect on the spiral mode. It does contain some expressions that are useful in the description of the effect of several loops on the spiral mode. Reference 5 correlates root-locus analysis with the equivalent stability-derivative approach in the description of single-sensor control loops. The discussion is limited to two specific feedback loops and is not primarily concerned with variable-stability aircraft applications.

This paper summarizes the results of an analysis of the influence of response feedback loops on the lateral-directional dynamics of a variable-stability transport aircraft. It is intended to fill a significant gap in the available literature by presenting fundamental information on the response feedback system, demonstrating some of the more successful analysis techniques, and discussing in detail the feedback loops commonly used in variable-stability aircraft. Somewhat unique is the range of feedback gain for the JetStar for which certain classical approximations are valid in describing the effect of a particular loop.

SYMBOLS

The units used for physical quantities in this paper are given, where applicable, in both the International System of Units (SI) and U. S. Customary Units. Factors relating the two systems are included in reference 6.

The body-axis system and sign conventions used in this paper are shown in figure 1.

A, B, C, D, E	coefficients of fourth-order algebraic equation
b	wing span, m (ft)
C_D	drag coefficient
C_l	rolling-moment coefficient
C_n	yawing-moment coefficient
C_Y	side-force coefficient
$C_{l_p} = \frac{\partial C_l}{\partial\left(\frac{pb}{2V}\right)}$	

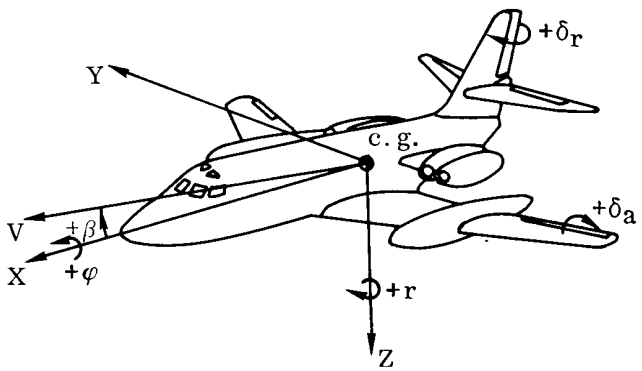

Figure 1.– Body-axis system and sign conventions.

$$C_{l_r} = \frac{\partial C_l}{\partial \left(\frac{rb}{2V}\right)}$$

$$C_{l_\beta} = \frac{\partial C_l}{\partial \beta}$$

$$C_{l_{\dot{\beta}}} = \frac{\partial C_l}{\partial \left(\frac{\dot{\beta} b}{2V}\right)}$$

$$C_{l_{\delta_a}} = \frac{\partial C_l}{\partial \delta_a}$$

$$C_{l_{\delta_r}} = \frac{\partial C_l}{\partial \delta_r}$$

$$C_{n_p} = \frac{\partial C_n}{\partial \left(\frac{pb}{2V}\right)}$$

$$C_{n_r} = \frac{\partial C_n}{\partial \left(\frac{rb}{2V}\right)}$$

$$C_{n_\beta} = \frac{\partial C_n}{\partial \beta}$$

$$C_{n_{\dot{\beta}}} = \frac{\partial C_n}{\partial \left(\frac{\dot{\beta} b}{2V}\right)}$$

$$C_{n_{\delta_a}} = \frac{\partial C_n}{\partial \delta_a}$$

$$C_{n_{\delta_r}} = \frac{\partial C_n}{\partial \delta_r}$$

$$C_{Y_r} = \frac{\partial C_Y}{\partial \left(\frac{rb}{2V}\right)}$$

$C_{Y_\beta} = \frac{\partial C_Y}{\partial \beta}$

$C_{Y_{\dot{\beta}}} = \frac{\partial C_Y}{\partial \left(\frac{\dot{\beta} b}{2V} \right)}$

$C_{Y_{\delta_r}} = \frac{\partial C_Y}{\partial \delta_r}$

e	natural log base
g	acceleration of gravity, m/sec^2 (ft/sec^2)
I_{XX}, I_{YY}, I_{ZZ}	moments of inertia referred to X, Y, and Z body axes, respectively, $kg\text{-}m^2$ ($slug\text{-}ft^2$)
I_{XZ}	product of inertia referred to X and Z body axes, $kg\text{-}m^2$ ($slug\text{-}ft^2$)
j	complex variable operator
$j\omega$	designation of imaginary axis of s-plane, rad/sec (deg/sec)
K	a constant

$L_p = \frac{\bar{q}Sb}{I_{XX}} \frac{b}{2V} C_{l_p}$

$L_r = \frac{\bar{q}Sb}{I_{XX}} \frac{b}{2V} C_{l_r}$

$L_\beta = \frac{\bar{q}Sb}{I_{XX}} C_{l_\beta}$

$L_{\dot{\beta}} = \frac{\bar{q}Sb}{I_{XX}} \frac{b}{2V} C_{l_{\dot{\beta}}}$

$L_{\delta_a} = \frac{\bar{q}Sb}{I_{XX}} C_{l_{\delta_a}}$

$L_{\delta_r} = \frac{\bar{q}Sb}{I_{XX}} C_{l_{\delta_r}}$

L_φ	artificially created stability derivative; rolling acceleration due to bank angle

m mass, kg (slugs)

$N_p = \frac{\bar{q}Sb}{I_{ZZ}} \frac{b}{2V} C_{n_p}$

$N_r = \frac{\bar{q}Sb}{I_{ZZ}} \frac{b}{2V} C_{n_r}$

$N_\beta = \frac{\bar{q}Sb}{I_{ZZ}} C_{n_\beta}$

$N_{\dot{\beta}} = \frac{\bar{q}Sb}{I_{ZZ}} \frac{b}{2V} C_{n_{\dot{\beta}}}$

$N_{\delta_a} = \frac{\bar{q}Sb}{I_{ZZ}} C_{n_{\delta_a}}$

$N_{\delta_r} = \frac{\bar{q}Sb}{I_{ZZ}} C_{n_{\delta_r}}$

N_φ artificially created stability derivative; yawing acceleration due to bank angle

p rolling angular velocity, rad/sec (deg/sec)

q pitching angular velocity, rad/sec (deg/sec)

$\bar{q}$ dynamic pressure, $\frac{1}{2}\rho V^2$, N/m^2 (lb/ft^2)

r yawing angular velocity, rad/sec (deg/sec)

S wing area, m^2 (ft^2)

s Laplace transform variable

u velocity component along X body axis, m/sec (ft/sec)

V true airspeed, m/sec (ft/sec)

v velocity component along Y body axis, m/sec (ft/sec)

w velocity component along Z body axis, m/sec (ft/sec)

$Y_r = \frac{\bar{q}S}{mV} \frac{b}{2V} C_{Y_r}$

$Y_\beta = \frac{\bar{q}S}{mV} C_{Y_\beta}$

$Y_{\dot{\beta}} = \frac{\bar{q}S}{mV} \frac{b}{2V} C_{Y_{\dot{\beta}}}$

$Y_{\delta_r} = \frac{\bar{q}S}{mV} C_{Y_{\delta_r}}$

X, Y, Z	body-axis coordinates
α	angle of attack, rad (deg)
β	angle of sideslip, positive for velocity vector toward right, rad (deg)
δ_a	total aileron deflection, $\delta_{a_{left}} - \delta_{a_{right}}$, positive for left aileron deflected trailing edge down, rad (deg)
δ_{a_p}	pilot aileron command, positive when commanding positive δ_a, rad (deg)
δ_r	rudder deflection, positive for trailing edge left, rad (deg)
δ_{r_c}	command to rudder actuator or aircraft transfer function, rad (deg)
δ_{r_p}	pilot rudder command, positive when commanding positive δ_r, rad (deg)
ζ_n	damping ratio of second-order dynamic response
ζ_φ	$\frac{\varphi}{\delta_a}(s)$ transfer-function numerator parameter
ζ_ψ	Dutch roll damping ratio
Θ	pitch-attitude angle, rad (deg)
ρ	mass density of air, kg/m^3 ($slugs/ft^3$)
σ	designation of real axis of s-plane
τ_r	roll mode time constant, sec
τ_s	spiral mode time constant, sec
φ	roll angle, rad (deg)

φ_A	actuator phase lag, rad (deg)
λ	arbitrary phase angle, rad (deg)
ψ	heading angle, rad (deg)
ω	frequency, rad/sec
ω_n	undamped natural frequency of a second-order dynamic response, rad/sec
ω_φ	$\frac{\varphi}{\delta_a}(s)$ transfer-function numerator parameter
ω_ψ	Dutch roll undamped natural frequency, rad/sec

Feedback loop and transfer-function nomenclature[1]:

$\frac{\delta_a}{p}$	feedback loop which commands aileron proportional to roll rate, and the actual value of feedback gain (e.g., $\frac{\delta_a}{p} = 5$ rad/rad/sec), rad/rad/sec (deg/deg/sec)
$\frac{\delta_a}{r}$	feedback loop which commands aileron proportional to yaw rate, and a gain value, rad/rad/sec (deg/deg/sec)
$\frac{\delta_a}{\beta}$	feedback loop which commands aileron proportional to angle of sideslip, and a gain value, rad/rad (deg/deg)
$\frac{\delta_a}{\varphi}$	feedback loop which commands aileron proportional to roll angle, and a gain value, rad/rad (deg/deg)
$\frac{\delta_r}{r}$	feedback loop which commands rudder proportional to yaw rate, and a gain value, rad/rad/sec (deg/deg/sec)
$\frac{\delta_r}{\beta}$	feedback loop which commands rudder proportional to angle of sideslip, and a gain value, rad/rad (deg/deg)
$\frac{\delta_r}{\dot{\beta}}$	feedback loop which commands rudder proportional to time derivative of sideslip angle, and a gain value, rad/rad/sec (deg/deg/sec)

[1]Values of feedback loop gains and transfer function ratios in this paper are the same in both the SI and U. S. Customary Units.

$\frac{\delta_r}{\delta_{r_c}}(s)$ actuator transfer function

$\frac{p}{\delta_a}(s)$ roll rate to aileron transfer function

$\left|\frac{\varphi}{\beta}(s)\right|_{\psi}$ magnitude of roll angle to sideslip-angle transfer function evaluated at the Dutch roll root

$\frac{\omega_\varphi}{\omega_\psi}$ handling-qualities parameter

$\frac{r}{\delta_r}(s)$ yaw rate to rudder transfer function

Subscript:

T trim value

A dot over a quantity indicates the differentiation with respect to time; a double dot indicates the second differentiation with respect to time.

Special notation:

basic relates quantity to unaugmented aircraft, no feedback gains

closed loop with at least one feedback gain $\neq 0$

effective including the augmentation of response feedback loops

open loop all feedback gains = 0, which results in a basic configuration

GENERAL DISCUSSION

In many cases the response feedback loops effectively augment the aerodynamic stability derivatives of the aircraft, hence the influence of these loops can be described by considering the usual effect of those particular stability derivatives on aircraft dynamics. However, some loops create aerodynamic stability derivatives that are nonexistent for the basic aircraft. The effect of these loops can be interpreted by noting the effect of the created stability derivatives. Where the classical approximations are not valid, root-locus diagrams and analog-computer results are used to describe the action of the loops on the airplane responses. These other methods are necessary when feedback gains are high enough to augment some aerodynamic stability derivatives which, because of their usual small contribution to a certain dynamic mode, are not considered in the usual approximations.

Since the response feedback system can often be described in terms of equivalent stability derivatives, the effects of these loops vary somewhat, depending on the characteristics of the aircraft being considered. The quantitative results in this paper were obtained for the GPAS from analytical studies of a Lockheed JetStar, an executive-type jet transport with aft-fuselage mounted engines. References to loop gain values should be indicative of values for other types of high-performance jet transports. Most large transports exhibit similar lateral-directional dynamics, which indicates similar transfer-function characteristics, and small variations in the basic aircraft transfer functions generally do not alter the dominant influence of a particular feedback loop. Thus, a particular loop described for the JetStar will have much the same effect on other aircraft in its class with some variation in the amount of feedback gain required to achieve certain closed-loop dynamics.

Since the individual feedback loops utilize the conventional aircraft control surfaces, the effectiveness of the loop is also a function of dynamic pressure and moments of inertia. Specific gains mentioned are valid only for a particular flight condition. Numerous references are made to flight condition, thus a code is used for convenience. Three parameters are written together in the following order: Mach number, weight, altitude (in thousands of meters (thousands of feet)). Thus, 0.55H6.1 denotes a Mach number of 0.55, heavy (17,236 kg (38,000 lb)), and 6100 meters (20,000 feet) altitude, and 0.23L0 denotes a Mach number of 0.23, light (10,886 kg (24,000 lb)), at sea level.

The particular feedback loops discussed herein were chosen because they are the most effective for varying aircraft dynamics and are used on other variable-stability aircraft. Most root-locus diagrams presented are for the 0.23L0 flight condition. The analysis was originally made for this case because it represented a low-dynamic-pressure condition, and hence gave information on minimum loop effectiveness. There is no other significance to the selection of this flight condition. Root-locus diagrams for this case are representative of those throughout the flight envelope. Where significant differences do occur, another root-locus diagram or special comment is included.

The response feedback loops analyzed are listed in the following table along with their estimated maximum gains, primary influence, and reasons for reaching a limit. These maximums were anticipated by the Cornell Aeronautical Laboratory on the basis of their experience with variable-stability aircraft and were used to predict the simulation capability of the GPAS. Actual limits can be determined only by flight test.

SUMMARY OF RESPONSE FEEDBACK LOOPS

Feedback loop	Primary derivative changed	Estimated maximum range of gain	Primary influence	Reasons for reaching estimated maximum
$\frac{\delta_r}{\beta}$	N_β	±10 rad/rad	Dutch roll frequency, directional stability	Structural instability and noise
$\frac{\delta_r}{\dot{\beta}_{vane}}$	$N_{\dot{\beta}}$	±1 rad/rad/sec	Dutch roll damping	Noise
$\frac{\delta_r}{r}$	N_r	±4 rad/rad/sec	Dutch roll damping	Sufficient for the task
$\frac{\delta_a}{\varphi}$	L_φ	±5 rad/rad	Roll-attitude stabilization	Sufficient for the task
$\frac{\delta_a}{p}$	L_p	±2 rad/rad/sec	Roll mode time constant	Structural instability and noise
$\frac{\delta_a}{r}$	L_r	±4 rad/rad/sec	Spiral mode time constant	Sufficient for the task
$\frac{\delta_a}{\beta}$	L_β	±10 rad/rad	Roll to sideslip ratio, dihedral effect	Noise

ANALYSIS OF SINGLE CONTROL LOOPS

In the following sections, two assumptions are made concerning the feedback loops that are analyzed:

1. The response sensors have no dynamics of their own. They yield a signal proportional to the response with no time lag.

2. The actuators are also considered to be ideal. Actuator dynamics are neglected.

These assumptions are made in order to simplify the analysis to the point where basic loop effects are not clouded by hardware-imposed restrictions.

Each feedback loop can be represented as shown in figure 2, in which the $\frac{\delta_r}{r}$ loop is used as an example. The commanded rudder δ_r is a combination of the pilot input δ_{r_p} and the rudder commanded by the feedback loop $r\left(\frac{\delta_r}{r}\right)$ as follows:

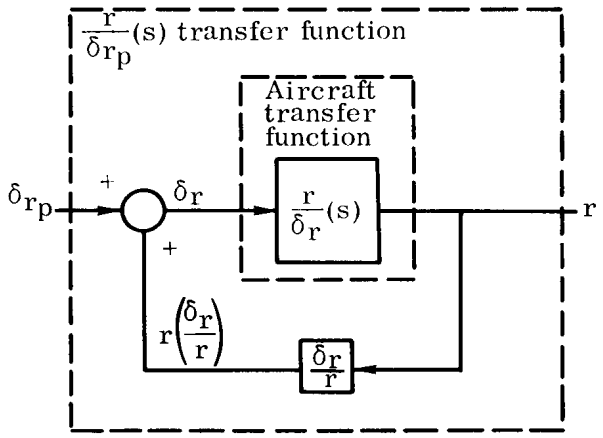

Figure 2.– Feedback-loop configuration.

$$\delta_r = \delta_{r_p} + r\left(\frac{\delta_r}{r}\right) \qquad (1)$$

Note that the feedback gain $\frac{\delta_r}{r}$ can be either positive or negative. The rudder deflection, then, is a function of the aircraft's yaw-rate response. The aircraft transfer function is a mathematical model used to describe the input-output relationship between an aircraft controller and an aircraft response. The $\frac{r}{\delta_r}$(s) transfer function is calculated from the equations of motion (appendix A). Substitution of equation (1) into the equations of motion will eliminate δ_r and add three new terms to the equations:

$$\left(\frac{\delta_r}{r}\right) Y_{\delta_r} r, \text{ augmenting } Y_r r$$

$$\left(\frac{\delta_r}{r}\right) L_{\delta_r} r, \text{ augmenting } L_r r$$

$$\left(\frac{\delta_r}{r}\right) N_{\delta_r} r, \text{ augmenting } N_r r$$

The $\frac{r}{\delta_{r_p}}(s)$ transfer function can be calculated from these modified equations and will be a function of the feedback gain $\frac{\delta_r}{r}$. The feedback loop will not affect all three terms equally but will depend on the relative magnitudes of Y_{δ_r}, L_{δ_r}, and N_{δ_r}. If, for example, $N_{\delta_r} \gg L_{\delta_r}$ and $N_{\delta_r} \gg Y_{\delta_r}$, the $\frac{\delta_r}{r}$ feedback loop would act almost entirely as an N_r augmentation loop. The equations will also be in terms of δ_{r_p} instead of δ_r.

It is apparent that the $\frac{\delta_r}{r}$ loop does affect the equations of motion and the $\frac{r}{\delta_{r_p}}(s)$ transfer function will also be affected. It might be asked, then, which of the other transfer functions are changed, and, since the transfer functions are usually presented in the form of one polynomial in s divided by another polynomial in s, whether the numerator or denominator or both will be a function of the feedback gain. The denominators of all lateral-directional transfer functions are identical. This polynomial, when set equal to zero, is referred to as the characteristic equation. The characteristic equation is altered by any feedback loop as shown in references 7 and 8. The effect of feedback loops on transfer-function numerators is not obvious (see, for example, ref. 9), but the following facts are noteworthy and can be easily proved by deriving particular transfer functions which fall into the categories mentioned:

1. The closed-loop transfer function resulting from feeding back a response variable to one control input has the same numerator as the open-loop transfer function. In other words, the numerator of the $\frac{r}{\delta_{r_p}}(s)$ transfer function with a $\frac{\delta_r}{r}$ feedback loop is identical to the numerator of the $\frac{r}{\delta_{r_p}}(s)$ transfer function with no feedbacks, which is, of course, the open-loop transfer function.

2. Loops which feed back some response variable to a particular control input will not alter the numerators of transfer functions relating any other response variable to that same control input. That is, the $\frac{\delta_r}{r}$ feedback loop will not alter the $\frac{\beta}{\delta_{r_p}}(s)$ or $\frac{\varphi}{\delta_{r_p}}(s)$ transfer function numerators.

3. It is possible to alter the numerator of a particular transfer function by feeding back a different response variable to a different control input. Thus, the numerator of the $\frac{\beta}{\delta_{a_p}}(s)$ transfer function will be altered by the $\frac{\delta_r}{r}$ feedback loop. It will not be altered by the $\zeta\frac{r}{\delta_a}$ feedback loop or the $\zeta\frac{\beta}{\delta_r}$ feedback loop.

This paper draws heavily from the interpretation of dynamic stability from s-plane considerations. These relationships are discussed in references 7 and 8 and in appendix B, which summarizes the application of root-locus results to dynamic stability analysis.

The $\frac{\delta_r}{r}$ Feedback Loop

The $\frac{\delta_r}{r}$ feedback loop, or yaw damper, is common in many aircraft. One convenient method of analyzing this loop is to consider the two-degree-of-freedom approximation to the Dutch roll. By including the feedback equation in the equations of motion in appendix A, the characteristic equation can be written approximately, as derived in appendix C, as

$$s^2 - \left[N_r + Y_\beta + \left(\frac{\delta_r}{r}\right) N_{\delta_r}\right]s + N_\beta + N_r Y_\beta + \left(\frac{\delta_r}{r}\right)\left(N_{\delta_r} Y_\beta - N_\beta Y_{\delta_r}\right) = 0 \qquad (2)$$

Comparing equation (2) with the standard form of the second-order approximation to the Dutch roll, $s^2 + 2\zeta_\psi \omega_\psi s + \omega_\psi^2 = 0$, results in

$$2\zeta_\psi \omega_\psi = -\left[N_r + Y_\beta + \left(\frac{\delta_r}{r}\right) N_{\delta_r}\right] \qquad (3)$$

$$\omega_\psi^2 = N_\beta + N_r Y_\beta + \left(\frac{\delta_r}{r}\right)\left(N_{\delta_r} Y_\beta - N_\beta Y_{\delta_r}\right) \qquad (4)$$

It is apparent from equations (3) and (4) that the $\frac{\delta_r}{r}$ loop will affect both the natural frequency and the damping ratio of the Dutch roll with varying degrees of effectiveness. For any given aircraft, numbers can be substituted into equations (3) and (4) to find how effective $\frac{\delta_r}{r}$ is in changing ζ_ψ and ω_ψ. For relatively small values of $\frac{\delta_r}{r}$, $\left(\frac{\delta_r}{r}\right)N_{\delta_r}$ is of the same magnitude as $N_r + Y_\beta$ for the JetStar at most flight conditions. Hence, for gain values of $\frac{\delta_r}{r}$ between 1 and 2.5 rad/rad/sec (deg/deg/sec), the $2\zeta_\psi\omega_\psi$ term is greatly changed. For the same range of gain, however, the $\left(\frac{\delta_r}{r}\right)\left(N_{\delta_r} Y_\beta - N_\beta Y_{\delta_r}\right)$ term is small compared to $N_\beta + N_r Y_\beta$. Therefore, little ω_ψ variation is to be expected for small $\frac{\delta_r}{r}$ gain values; thus, in equation (3) ζ_ψ will be primarily affected. By neglecting the ω_ψ variation and noting that $N_\beta \gg N_r Y_\beta$ for the JetStar as well as most transport aircraft, equation (2) becomes

$$s^2 - \left[N_r + Y_\beta + \left(\frac{\delta_r}{r}\right) N_{\delta_r}\right]s + N_\beta = 0 \qquad (5)$$

Thus, the $\frac{\delta_r}{r}$ loop is almost entirely a Dutch roll damping loop for relatively small gain values, on the basis of the classical two-degree-of-freedom Dutch roll approximation.

The root-locus technique can be used to relate the dynamic characteristics of the aircraft directly to the value of the feedback gain $\frac{\delta_r}{r}$. Figure 3 is typical of most Jet-Star flight conditions. The locus shown is for a positive yaw rate fed back as a

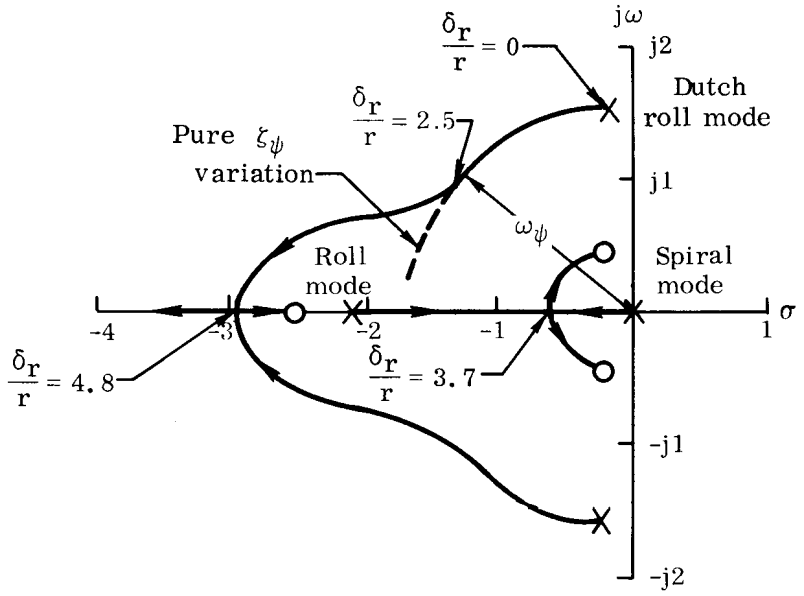

Figure 3.– Root locus for the $\frac{\delta_r}{r}$ loop at 0.23L0.
(Gain values in rad/rad/sec.)

positive rudder input. The pole locations for $\frac{\delta_r}{r} = 0$ represent the open-loop aircraft. For $\frac{\delta_r}{r} < 2.5$ rad/rad/sec, the Dutch roll damping ratio is affected, with little change in ω_ψ, as the previous discussion predicted. The Dutch roll approximation does not adequately describe the effect of the feedback loop for gains greater than 2.5 rad/rad/sec. Equation (5), then, is valid only for $\frac{\delta_r}{r} < 2.5$ rad/rad/sec. Above this value of gain the Dutch roll damping ratio is still increased, but a marked increase in frequency is also evident. Hardware limitations (table, page 9) are expected to restrict the maximum feedback gain to about ±4 rad/rad/sec for the JetStar, so for moderate gain values the feedback loop can be considered as a damping loop for the Dutch roll. The dashed line in figure 3 shows how the root-locus diagram would look if the feedback loop had a pure effect on the Dutch roll damping ratio.

The $\frac{\delta_r}{r}$ feedback loop has some other noteworthy effects on the aircraft dynamics. As the Dutch roll becomes more stable, the spiral mode becomes more stable. (For a few flight conditions, 0.75L20, for instance, the zero locations are such that spiral divergence results.) The roll and spiral modes merge for $\frac{\delta_r}{r} = 3.7$ rad/rad/sec, and for greater gain values a lateral phugoid mode exists. It should be noted that this mode may not be attainable in practice, since a gain of 3.7 rad/rad/sec is near the expected maximum.

The root locus for the opposite sign of the feedback gain is shown in figure 4. Since root-locus diagrams are symmetrical with respect to the real axis, only the top half is shown in this and succeeding diagrams. For very low feedback gain levels the spiral mode becomes divergent. As the gain level is increased, the Dutch roll becomes divergent as a result of the decrease in damping ratio to zero. The roll mode is virtually unaffected by the feedback loop in this case. If this loop is to be used to decrease Dutch roll damping, some means must be provided to maintain spiral stability.

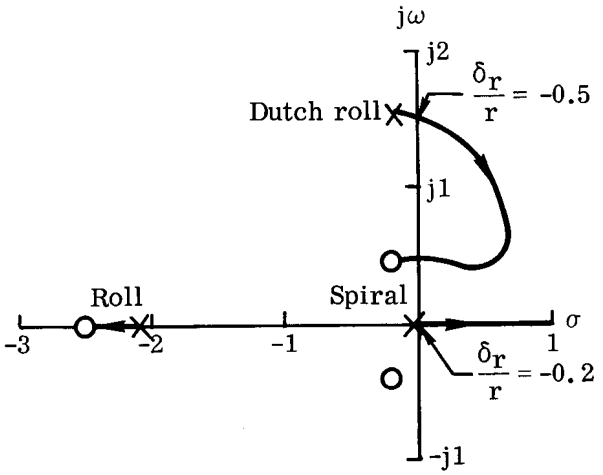

Figure 4.– Root locus for the $-\frac{\delta_r}{r}$ loop at 0.23L0. (Gain values in rad/rad/sec.)

The root locus for a higher dynamic pressure flight condition, 0.55H6.1 (0.55H20), is presented in figure 5. The dynamic pressure at this flight condition is 9911 N/m^2 (206 lb/ft^2), compared with 3735 N/m^2 (78 lb/ft^2) at 0.23L0. The roll mode time constant is larger, hence the pole is nearer the imaginary axis than before. The Dutch roll locus is nearly a perfect quadrant of a circle, which means that for an increased $\frac{\delta_r}{r}$ gain an increase in ζ_ψ can be realized with virtually no change in Dutch roll natural frequency for ζ_ψ between 0 and 1. The maximum value of gain for which no change in ω_ψ occurs is 2.1 rad/rad/sec, approximately the value for which ω_ψ started to be affected at the 0.23L0 flight condition, even though the root locus is slightly different. The first breakaway into a lateral phugoid occurs with an attainable feedback gain, 2.3 rad/rad/sec. However, the high damping ratio ($\zeta_n > 0.9$) makes it difficult to detect. The second breakaway occurs for a gain of 4 rad/rad/sec, which is the expected maximum gain.

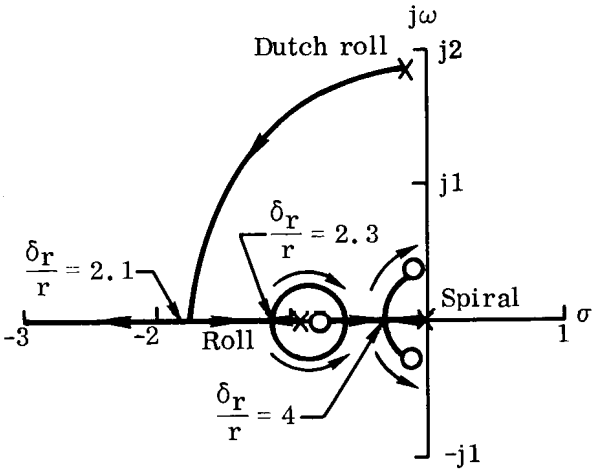

Figure 5.– Root locus for the $\frac{\delta_r}{r}$ loop at 0.55H6.1 (0.55H20). (Gain values in rad/rad/sec.)

One of the practical problems in using the $\frac{\delta_r}{r}$ loop occurs during a steady turn. For the stabilizing sense of the gain, the $\frac{\delta_r}{r}$ loop commands a rudder deflection to oppose any yaw rate. In a turn this means that an increased amount of rudder-pedal input by the pilot is required to maintain some steady yaw rate. The usual method of eliminating this problem is by inserting a "washout" circuit in the $\frac{\delta_r}{r}$ feedback loop,

which reduces the effectiveness of the loop at low frequencies. Hence, during a steady turn, the yaw-rate feedback gain is zero.

The $\frac{\delta_r}{\dot{\beta}}$ Feedback Loop

For certain wings-level maneuvers, $\dot{\beta}$ can be assumed to be approximately equal to $-r$. It would seem, then, that the effect of the $\pm\frac{\delta_r}{\dot{\beta}}$ loop is similar in its effect to that of the $\mp\frac{\delta_r}{r}$ loop. Comparison of the root-locus diagrams in figures 3 and 6 shows the similarity. An expression can be derived relating the feedback $\frac{\delta_r}{\dot{\beta}}$ to a Dutch roll characteristic and to aerodynamic stability derivatives of the basic aircraft. This relationship is shown in the following equation:

$$\frac{\delta_r}{\dot{\beta}} = \frac{2\zeta_\psi \omega_\psi + N_r + Y_\beta}{N_{\delta_r} + Y_{\delta_r}\left(N_r + 2\zeta_\psi\omega_\psi\right)} \tag{6}$$

The derivation of this equation and the conditions of validity (appendix D) illustrate a useful approach which results in similar expressions. Equation (6) allows the gain to be calculated that will yield the value of $2\zeta_\psi\omega_\psi$ desired.

The root-locus plot of figure 6 is for the feedback configuration commanding a negative δ_r for a positive $\dot{\beta}$. The figure shows that the $\frac{\delta_r}{\dot{\beta}}$ loop alters the Dutch roll damping ratio with little effect on ω_ψ, hence in equation (6) the selection of some $2\zeta_\psi\omega_\psi$ implies the choice of a particular ζ_ψ with ω_ψ remaining nearly constant at its open-loop value. Equation (6) assumes that ω_ψ does not vary, and figure 6 indicates that this assumption is good for $\left|\frac{\delta_r}{\dot{\beta}}\right| < 2.5$ rad/rad/sec. Over a fairly large range of gain where ζ_ψ is varying rapidly $\left(\left|\frac{\delta_r}{\dot{\beta}}\right|$ between 0 and 2 rad/rad/sec$\right)$, the roll and spiral modes are not influenced as much as when $\frac{\delta_r}{r}$ is used.

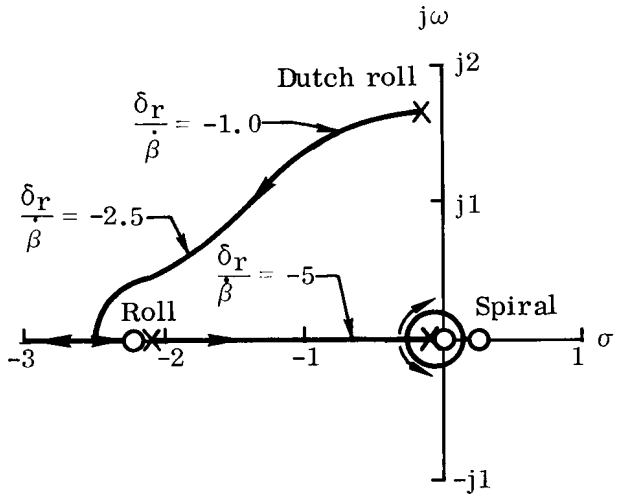

Figure 6.– Root locus for the $-\frac{\delta_r}{\dot{\beta}}$ loop at 0.23L0.

(Gain values in rad/rad/sec.)

If $\dot{\beta}$ is obtained by differentiating β as measured by a vane, the loop may be noisy, thus limiting the feedback gain to relatively small values. Gains of much more than 1 rad/rad/sec are not to be expected with a $\dot{\beta}$ signal derived by differentiation; hence, equation (6) is applicable for all practical gain values. To

circumvent the noisy $\dot{\beta}$ vane signal, $\dot{\beta}$ may be synthesized by measuring bank angle, yaw rate, and lateral acceleration and solving a simplified side-force equation (ref. 10). The resulting $\dot{\beta}$ will be less susceptible to gust disturbances and will allow a higher feedback gain to be used.

Reversing the sign of the feedback gain results in the root-locus diagram in figure 7. The roll and spiral modes are still unaffected. The Dutch roll becomes divergent for $\frac{\delta_r}{\dot{\beta}} = 0.3$ rad/rad/sec. The Dutch roll damping ratio is again altered with little change in ω_ψ. Comparison of the root-locus diagrams of the $\frac{\delta_r}{r}$ and $\frac{\delta_r}{\dot{\beta}}$ loops (figs. 2, 3, 5, and 6) shows the latter to be more nearly a pure Dutch roll damping loop, in that the roll and spiral modes are not influenced as significantly as they are with the $\frac{\delta_r}{r}$ feedback loop.

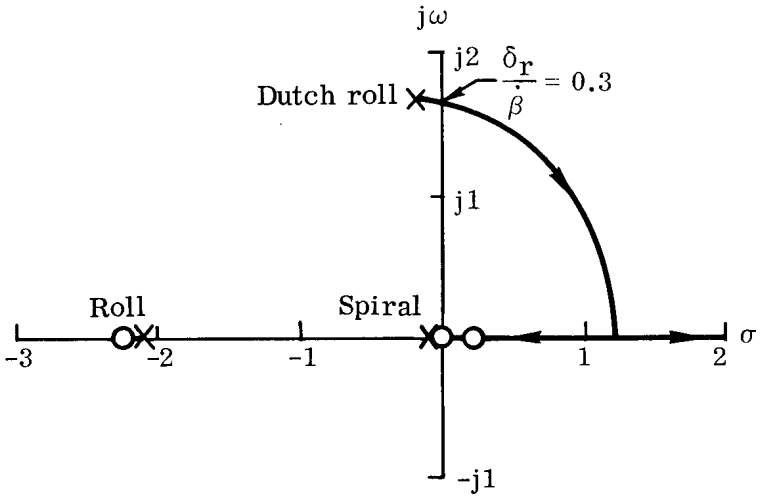

Figure 7.– Root locus for the $\frac{\delta_r}{\dot{\beta}}$ loop at 0.23L0.
(Gain values in rad/rad/sec.)

The $\frac{\delta_r}{\dot{\beta}}$ loop adds the following three terms to the equations of motion:

$$\left(\frac{\delta_r}{\dot{\beta}}\right) Y_{\delta_r}\dot{\beta}$$

$$\left(\frac{\delta_r}{\dot{\beta}}\right) L_{\delta_r}\dot{\beta}$$

$$\left(\frac{\delta_r}{\dot{\beta}}\right) N_{\delta_r}\dot{\beta}$$

These terms may be thought of as augmenting the three aerodynamic stability derivatives $Y_{\dot{\beta}}$, $L_{\dot{\beta}}$, and $N_{\dot{\beta}}$. These stability derivatives do not appear in the equations of motion for the JetStar (appendix A) because of their extremely small contribution. The $\frac{\delta_r}{\dot{\beta}}$ loop, then, can be regarded as actually creating the three derivatives, although they do exist for the basic JetStar. In perturbation-type maneuvers, these three derivatives have effects on lateral-directional dynamics similar to those of Y_r, L_r, and N_r.

The $\frac{\delta_r}{\beta}$ Feedback Loop

Angle of sideslip is detected and fed back as a rudder command to form the $\frac{\delta_r}{\beta}$ loop. The two-degree-of-freedom approximation to the Dutch roll is derived (appendix C) by writing an auxiliary equation similar to equation (1) and then solving for the characteristic equation as follows:

$$s^2 - \left[N_r + Y_\beta + \left(\frac{\delta_r}{\beta}\right) Y_{\delta_r}\right] s + N_\beta + \left(\frac{\delta_r}{\beta}\right) N_{\delta_r} = 0 \qquad (7)$$

For small values of $\frac{\delta_r}{\beta}$, the $\left(\frac{\delta_r}{\beta}\right) Y_{\delta_r}$ term is small compared to $N_r + Y_\beta$. The term $\left(\frac{\delta_r}{\beta}\right) N_{\delta_r}$, on the other hand, is comparable to N_β, hence the Dutch roll frequency will be primarily affected. When $\frac{\delta_r}{\beta}$ is of the proper sign to increase ω_ψ, the total system damping $2\zeta_\psi \omega_\psi$ will increase. The two-degree-of-freedom approximation (eq. (7)) is generally good for flight conditions of the JetStar where trim angle of attack is small. If this is true, the following expression can be written relating the Dutch roll frequency and the feedback gain $\frac{\delta_r}{\beta}$:

$$\frac{\delta_r}{\beta} = \frac{\omega_\psi^2 - N_\beta}{N_{\delta_r}} \qquad (8)$$

The N_β approximation for ω_ψ^2 is not satisfactory for large trim angles of attack. It is necessary to use a more complete expression for ω_ψ^2 which includes the term $\alpha_T L_\beta$, since this term is significant for large α_T.

Note that the $\frac{\delta_r}{\beta}$ loop acts as an effective N_β, also augmenting Y_β and L_β to a lesser degree, through the terms $\frac{\delta_r}{\beta}\left(N_{\delta_r}\right)$, $\frac{\delta_r}{\beta}\left(Y_{\delta_r}\right)$, and $\frac{\delta_r}{\beta}\left(L_{\delta_r}\right)$, respectively.

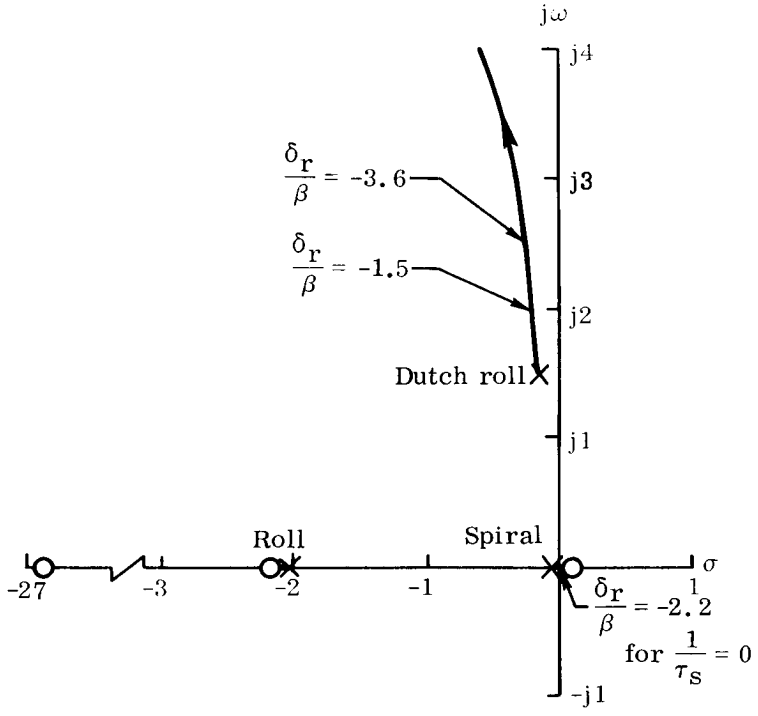

Figure 8.– Root locus for the $-\frac{\delta_r}{\beta}$ loop at 0.23L0.

(Gain values in rad/rad.)

A typical root-locus diagram for the JetStar is shown in figure 8. The locus represents the configuration in which positive β commands negative δ_r. The roll and spiral modes are altered very little. There is some slight spiral destabilization, but even for very high gain the closed-loop root can be no farther into the right half of the complex plane than the open-loop zero. For the JetStar, this means that the time to double amplitude for the divergent term is no less than 40 seconds for any flight condition when the $-\frac{\delta_r}{\beta}$ loop is being used alone.

The effect on the Dutch roll is of primary importance, and the poles move in the manner predicted analytically, following a line of

nearly constant $\zeta_\psi \omega_\psi$. Since the Dutch roll mode poles are usually lightly damped for this class of aircraft, the small increase in $\zeta_\psi \omega_\psi$ caused by $\left(\frac{\delta_r}{\beta}\right) Y_{\delta_r}$ usually results in the locus following a line of constant ζ_ψ. The Dutch roll undamped natural frequency ω_ψ is shown as a function of $\frac{\delta_r}{\beta}$ in figure 9. The plot is fairly linear for $\left|\frac{\delta_r}{\beta}\right| < 6$ rad/rad. Above this gain value, $\frac{\delta_r}{\beta}$ becomes less effective in increasing ω_ψ in the higher gain ranges. Practical considerations restrict $\left|\frac{\delta_r}{\beta}\right|$ to a maximum value not much greater than 10 rad/rad. The plot indicates that the effort required to increase the upper limit of the gain from that in table I might not be justified in light of the small increase realized in ω_ψ.

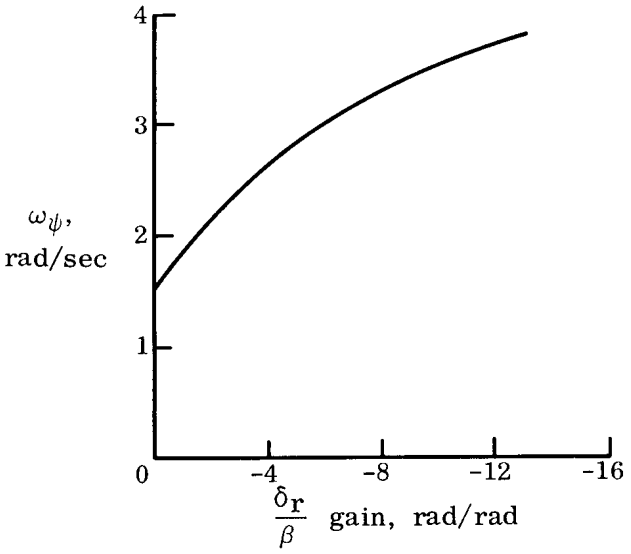

Figure 9.– Variation of ω_ψ with the $\frac{\delta_r}{\beta}$ feedback gain at 0.23L0.

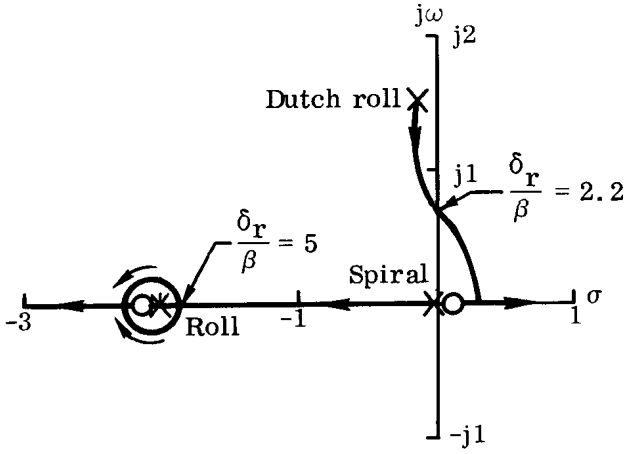

Figure 10.– Root locus for the $\frac{\delta_r}{\beta}$ loop at 0.23L0.
(Gain values in rad/rad.)

Reversing the sign of the feedback gain results in the root locus of figure 10. The Dutch roll frequency is reduced, and at the same time the damping ratio decreases. For $\left|\frac{\delta_r}{\beta}\right| > 2.2$ rad/rad the Dutch roll is unstable. The spiral mode is stabilized. The roll and spiral modes merge and form an oscillatory mode. This mode may not be possible to attain in practice because of Dutch roll instability.

It has been noted from figure 8 that the $\frac{\delta_r}{\beta}$ loop would change the total damping of the system very little. Figure 10 indicates that $2\zeta_\psi \omega_\psi$ decreases rapidly and goes to zero for a fairly low value of feedback gain. This indicates that the two-degree-of-freedom approximation is no longer a valid representation of the Dutch roll. From equation (7) it is noted that

$$2\zeta_\psi \omega_\psi = -N_r - Y_\beta - \left(\frac{\delta_r}{\beta}\right) Y_{\delta_r} \tag{9}$$

By substituting actual values for the stability derivatives, it is found that for $\frac{\delta_r}{\beta} = 2.2$ rad/rad, $\zeta_\psi \omega_\psi = 0.16$. The root locus, however, shows neutral stability. In this gain area the effective $\left|\frac{L_\beta}{N_\beta}\right|$ ratio is high. Reference 5 discusses conditions of validity for the $2\zeta_\psi \omega_\psi$ approximation. For large $\left|\frac{L_\beta}{N_\beta}\right|$ ratios the approximation given by equation (9) is not valid.

The primary influence of $\frac{\delta_r}{\beta}$ on the aircraft dynamics, that of changing ω_ψ alone, prevails for the stabilizing sense of the gain. Since the response feedback system works through the aerodynamic control derivatives, the effectiveness of the loops is a function of dynamic pressure. This dependency is shown by writing the expression for ω_ψ^2 as

$$\omega_\psi^2 = \frac{\bar{q}Sb}{I_{ZZ}}\left[C_{n_\beta} + \left(\frac{\delta_r}{\beta}\right) C_{n_{\delta_r}}\right] \tag{10}$$

It is evident from this equation that, for a given $\frac{\delta_r}{\beta}$ gain, ω_ψ^2 is directly proportional to dynamic pressure for regions of the flight envelope where C_{n_β} and $C_{n_{\delta_r}}$ are constant. The ratio between the closed loop ω_ψ^2 and the open loop ω_ψ^2, however, will be constant in this region for a given $\frac{\delta_r}{\beta}$ gain value, as shown by forming the ratio

$$\frac{\omega_\psi^2 \text{ closed loop}}{\omega_\psi^2 \text{ open loop}} = \frac{C_{n_\beta} + \left(\frac{\delta_r}{\beta}\right) C_{n_{\delta_r}}}{C_{n_\beta}} \tag{11}$$

The $\frac{\delta_a}{p}$ Feedback Loop

This feedback loop senses roll rate and commands aileron deflection proportionately. By writing an auxiliary equation similar to equation (1) and substituting it into the equations of motion (appendix A), it is noted that two new terms appear:

$$\left(\frac{\delta_a}{p}\right) L_{\delta_a} p, \text{ augmenting } L_p p$$

$$\left(\frac{\delta_a}{p}\right) N_{\delta_a} p, \text{ augmenting } N_p p$$

For the transport class of aircraft, L_{δ_a} is usually very much greater than N_{δ_a} so that the $\frac{\delta_a}{p}$ loop influences the effective L_p almost entirely. The aerodynamic stability derivative L_p is strongly related to the roll mode time constant. In fact, the

usual approximation, which is good for all JetStar flight conditions, is

$$\tau_r = -\frac{1}{L_{p(\text{effective})}} \tag{12}$$

Hence, the $\frac{\delta_a}{p}$ loop exercises strong and direct control over the roll mode time constant. The $\frac{\delta_a}{p}$ gain value must be relatively large before N_p augmentation is significant, compared with the strong influence on the effective L_p through L_{δ_a}.

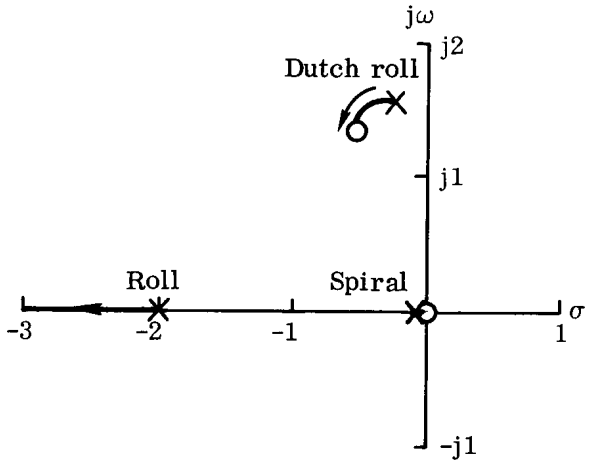

Figure 11.– Root locus for the $-\frac{\delta_a}{p}$ loop at 0.23L0.

(Gain values in rad/rad/sec.)

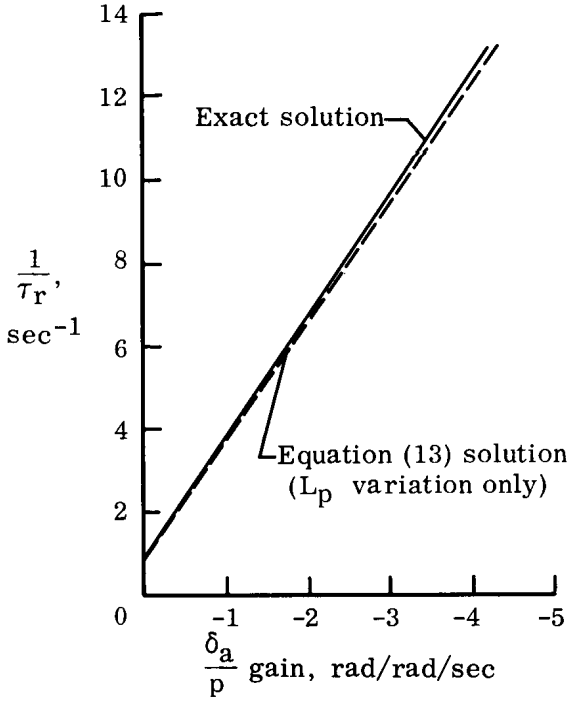

Figure 12.– Comparison of exact solution with equation (13) solution.

The root-locus diagram for the $-\frac{\delta_a}{p}$ loop is shown in figure 11. The spiral mode remains unchanged, and even high gains do not noticeably modify Dutch roll dynamics. The roll mode is stabilized. By using equation (12), the $\frac{\delta_a}{p}$ gain required for a particular roll mode time constant can be calculated to be

$$\frac{\delta_a}{p} = -\frac{\frac{1}{\tau_r} + L_p}{L_{\delta_a}} \tag{13}$$

The accuracy of equation (13) is shown in figure 12. The solid line represents the roll mode time constants resulting from a variation of $\frac{\delta_a}{p}$ obtained from an exact solution to the equations of motion for the 0.55H6.1 (0.55H20) flight condition. The dashed line represents the roll mode time constants and associated $\frac{\delta_a}{p}$ gains obtained from equation (13) which assumes only L_p augmentation. The close agreement shows the almost sole dependency of τ_r on L_p and indicates that equation (13) is a good approximation for the JetStar.

For a positive $\frac{\delta_a}{p}$ gain, the root locus of figure 13 results. The roll mode is now destabilized. The roll and spiral modes form a lateral phugoid as

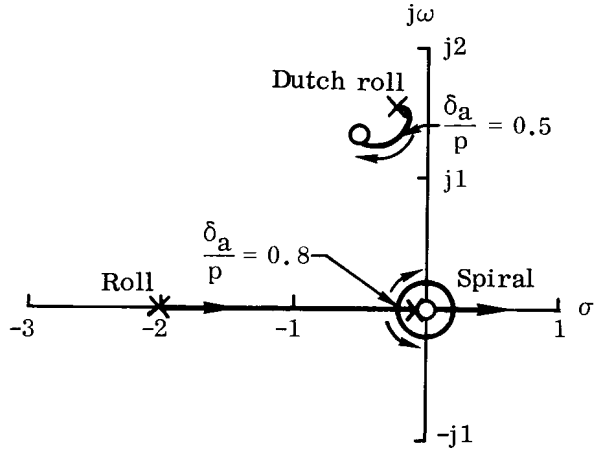

Figure 13.– Root locus for the $\frac{\delta_a}{p}$ loop at 0.23L0. (Gain values in rad/rad/sec.)

$\frac{\delta_a}{p}$ increases and eventually become unstable. The Dutch roll frequency is affected slightly, but the damping ratio is decreased noticeably.

For roll-mode analysis of the JetStar, the complex pole and zero pairs can be deleted without invalidating the locus on the real axis. This is equivalent to writing the open loop $\frac{p}{\delta_a}(s)$ transfer function

$$\frac{p}{\delta_a}(s) = \frac{Ks\left(s^2 + 2\zeta_\varphi\omega_\varphi s + \omega_\varphi{}^2\right)}{\left(s + \frac{1}{\tau_r}\right)\left(s + \frac{1}{\tau_s}\right)\left(s^2 + 2\zeta_\psi\omega_\psi s + \omega_\psi{}^2\right)} \qquad (14)$$

and noting that for the JetStar the two second-order terms are close to cancellation. This fact can be interpreted in terms of the handling-qualities ratio $\frac{\omega_\varphi}{\omega_\psi}$. For the JetStar and similarly configured transport aircraft, this ratio is approximately 1. The complex pole and zero will be very close to each other, depending on how close the ratio $\frac{\zeta_\varphi}{\zeta_\psi}$ is to 1. Thus, the Dutch roll poles will usually close on the complex zeros, not influencing the locus on the real axis.

The $\frac{\delta_a}{\beta}$ Feedback Loop

This feedback loop commands aileron deflection proportional to angle of sideslip. The aerodynamic stability derivatives L_β and N_β will be modified through the following new terms:

$$\left(\frac{\delta_a}{\beta}\right)L_{\delta_a\beta}, \text{ augmenting } L_{\beta\beta}$$

$$\left(\frac{\delta_a}{\beta}\right)N_{\delta_a\beta}, \text{ augmenting } N_{\beta\beta}$$

For the JetStar and similar aircraft, L_{δ_a} is usually much greater in magnitude than N_{δ_a}, hence, L_β augmentation will dominate. The influence of this loop varies more from one flight condition to another than the loops previously discussed but generally has a strong influence on the spiral mode and a noticeable effect on the Dutch roll mode. The action of this loop in providing a rolling moment due to sideslip is recognized as the dihedral effect. When L_β is increased negatively, the spiral mode is generally stabilized and the Dutch roll mode destabilized.

A representative root-locus diagram for the $-\frac{\delta_a}{\beta}$ loop is shown in figure 14. The exact shape of the locus for different flight conditions varies somewhat because of the drastic variation in $\frac{\beta}{\delta_a}(s)$ transfer function zeros. The figure shows the spiral mode being stabilized and the Dutch roll being destabilized, as is predicted from L_β considerations alone. The Dutch roll mode usually goes unstable for $\frac{\delta_a}{\beta}$ gains between -10 and -20 rad/rad. The frequency at which this occurs may be larger or smaller than the basic Dutch roll frequency. Figure 14 shows the root locus for a moderate $\bar{q}$ flight condition (9911 N/m^2 (207 lb/ft^2)), where $\frac{\delta_a}{\beta}$ increases the Dutch roll frequency. For the 0.75L6.1 (0.75L20) flight condition ($\bar{q}$ = 18,338 N/m^2 (383 lb/ft^2)) the Dutch roll goes unstable at a frequency slightly lower than the basic Dutch roll frequency. Depending on the relative locations of the spiral mode pole and its associated zero on the real axis, the $\frac{\delta_a}{\beta}$ loop will influence spiral stability with varying degrees of effectiveness.

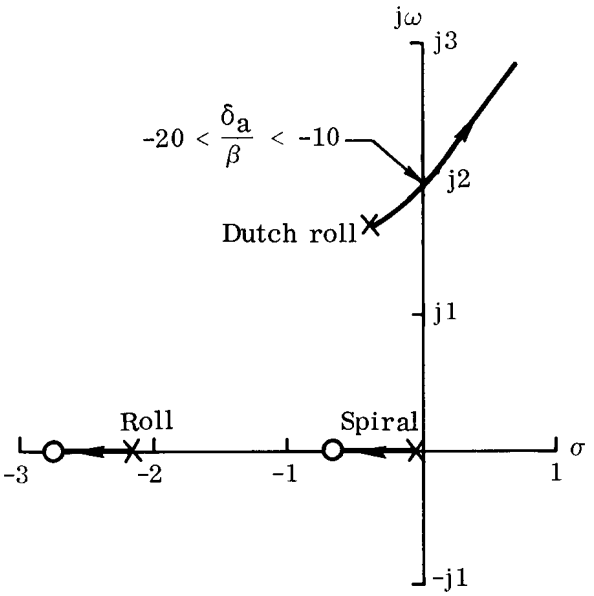

Figure 14.– Root locus for the $-\frac{\delta_a}{\beta}$ loop (typical).
(Gain values in rad/rad.)

Figure 15 shows a typical root-locus diagram for a positive $\frac{\delta_a}{\beta}$. The Dutch roll is stabilized (ζ_ψ increased), and the spiral mode is destabilized. The exact shape of the Dutch roll locus again is subject to flight condition, and for some higher dynamic pressures the Dutch roll frequency increases for the positive $\frac{\delta_a}{\beta}$ gain. For a realistic range of gain, $\left|\frac{\delta_a}{\beta}\right| < 10$ rad/rad (table, pg. 9), the Dutch roll dynamics are definitely affected, but the $\frac{\delta_a}{\beta}$ loop is not nearly as effective in changing ω_ψ or ζ_ψ as the $\frac{\delta_r}{\beta}$ (figs. 8 and 10) and $\frac{\delta_r}{r}$ (figs. 3 and 4) loops, respectively.

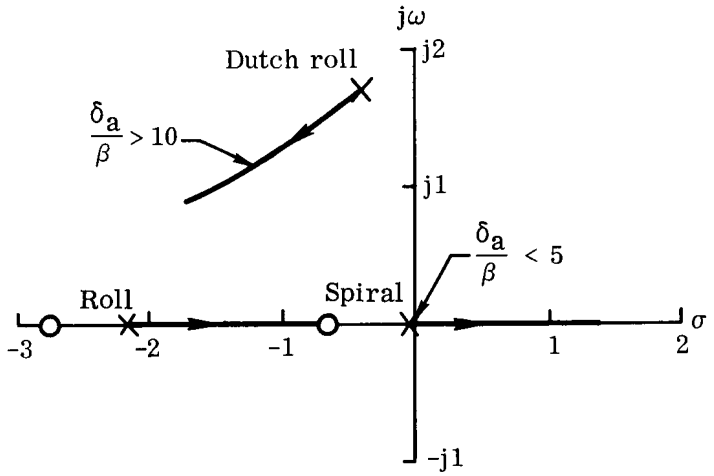

Figure 15.– Root locus for the $\frac{\delta_a}{\beta}$ loop (typical).
(Gain values in rad/rad.)

The $\frac{\delta_a}{r}$ Feedback Loop

The $\frac{\delta_a}{r}$ loop commands aileron deflection proportional to yaw rate. It is not one of the primary control loops that would be used alone but could find applications in multiloop combinations or in special cases. By augmenting N_r and L_r, this loop would be expected to alter Dutch roll damping.

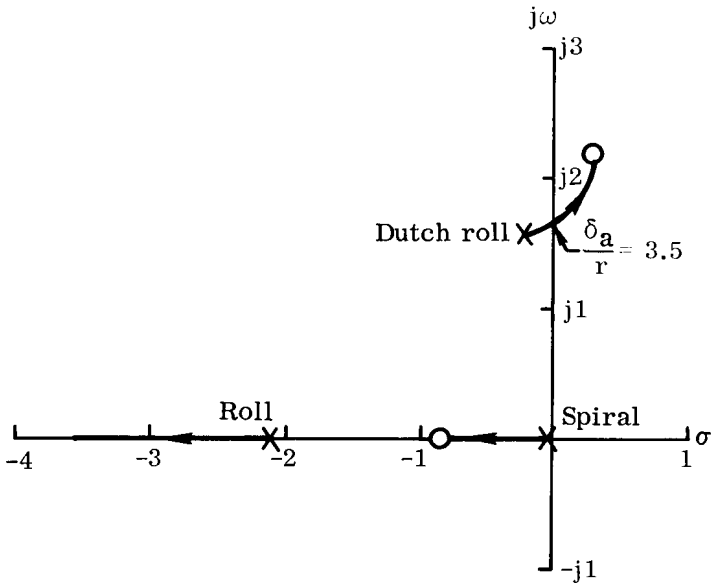

Figure 16.– Root locus for the $\frac{\delta_a}{r}$ loop at 0.23L0.
(Gain values in rad/rad/sec.)

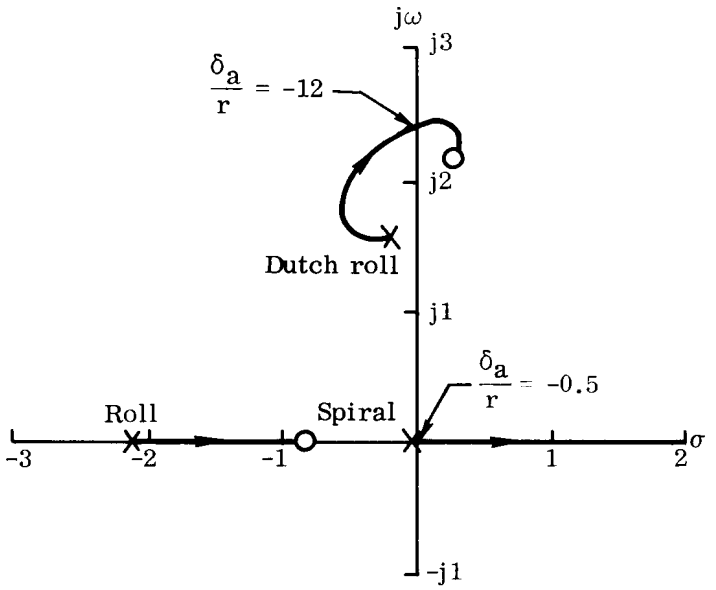

Figure 17.– Root locus for the $-\frac{\delta_a}{r}$ loop at 0.23L0.
(Gain values in rad/rad/sec.)

A representative root-locus diagram is shown in figure 16. For the JetStar, the complex zeros are generally in the right half of the plane for all but high dynamic pressure flight conditions. Relatively small values of feedback gain will cause Dutch roll instability. The spiral mode is stabilized as the effective L_r is decreased.

Reversing the sign of the feedback results in the root locus of figure 17. The spiral mode is divergent for very small gain values, usually less than 0.5 rad/rad/sec for most flight conditions. The spiral instability occurs for much smaller gain values than does Dutch roll instability, thus making use of this loop alone to alter Dutch roll effects impractical.

The $\frac{\delta_a}{\varphi}$ Feedback Loop

The $\frac{\delta_a}{\varphi}$ loop, commanding aileron proportional to bank angle, is somewhat distinctive in that it creates two aerodynamic stability derivatives that are nonexistent for the basic aircraft:

$\left(\frac{\delta_a}{\varphi}\right) L_{\delta_a \varphi}$, creating $L_{\varphi\varphi}$

$\left(\frac{\delta_a}{\varphi}\right) N_{\delta_a \varphi}$, creating $N_{\varphi\varphi}$

The root locus for the $-\frac{\delta_a}{\varphi}$ loop is shown in figure 18. The pole-zero configuration of figure 18 is identical to that of the $-\frac{\delta_a}{p}$ root locus (fig. 11) except that there is no zero at the origin. The spiral mode is stabilized and the roll mode destabilized. Dutch roll dynamics are affected very little. This loop can be used to create a low-frequency mode commonly referred to as the lateral phugoid. Increasing the feedback gain causes the roll and spiral modes to merge and form an oscillatory pair. The gain at breakaway varies with flight condition and is -0.3 rad/rad for the 0.23L0 condition. This loop is useful in itself in stabilizing the spiral mode or in conjunction with other loops in stabilizing the spiral mode without interfering with the Dutch roll dynamics.

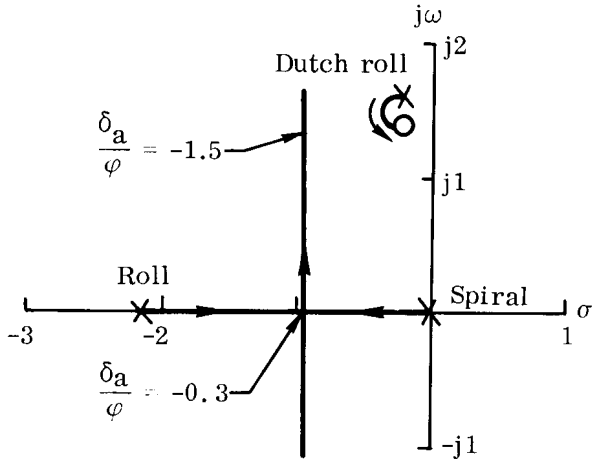

Figure 18.– Root locus for the $-\frac{\delta_a}{\varphi}$ loop at 0.23L0. (Gain values in rad/rad.)

Relating the spiral pole location to the feedback gain is not easily done because the spiral root cannot be simply expressed in terms of stability derivatives. When the characteristic equation of the system is written as

$$As^4 + Bs^3 + Cs^2 + Ds + E = 0 \tag{15}$$

it is possible to approximate the spiral root in terms of the coefficients of equation (15). If the assumption is made that a single-order root exists that is much smaller than any of the other roots, a good approximation to this root is

$$\frac{1}{\tau_s} \simeq \frac{E}{D} \tag{16}$$

By writing the complete characteristic equation from the set of lateral-directional equations in appendix A, including the auxiliary feedback equation, in the form of equation (15), the $\frac{E}{D}$ term can be formed as

$$\frac{E}{D} \simeq \frac{1}{\tau_s} \simeq \frac{\frac{g}{V_T}\left(L_\beta N_r - L_r N_\beta\right) - \left(\frac{\delta_a}{\varphi}\right) L_{\delta_a} N_\beta}{L_\beta N_p - L_p N_\beta - \frac{g}{V_T} L_\beta + \left(\frac{\delta_a}{\varphi}\right)\left[L_{\delta_a}(N_r + Y_\beta)\right]} \tag{17}$$

The derivation of equation (17) is presented in appendix E. For the aircraft without any feedback loops, $\frac{E}{D}$ is usually very small. The balance between $L_\beta N_r$ and $L_r N_\beta$

determines the sign of the fraction and, hence, determines if the spiral root is convergent or divergent. Investigation of relative magnitudes of terms in the numerator and denominator indicates that a very small variation of $\frac{\delta_a}{\varphi}$ is required to control the spiral mode.

In appendix E, the N_φ terms, $\left(\frac{\delta_a}{\varphi}\right)N_{\delta_a}$, were much smaller than the L_φ terms, $\left(\frac{\delta_a}{\varphi}\right)L_{\delta_a}$, and so were neglected. Thus, the $\frac{\delta_a}{\varphi}$ loop acts as though it creates an L_φ alone. However, it is important to note that this does not imply that an equivalent N_φ will not affect the spiral mode. If N_φ can be created where L_φ is insignificant, such as with a $\frac{\delta_r}{\varphi}$ loop or with wing-tip drag surfaces, spiral stability will be greatly affected, as shown in reference 4.

The $\frac{\delta_a}{\varphi}$ loop induces the derivative N_φ with the conventional aileron control surface, through N_{δ_a}, which is a very small number for the JetStar. This feedback loop can also be used to destabilize the spiral mode by reversing the sign of the feedback gain. The root locus for this case is shown in figure 19. The roll mode is now stabilized, and the value of $\frac{\delta_a}{\varphi}$ for which the spiral mode is divergent is small, usually less than 0.05 rad/rad.

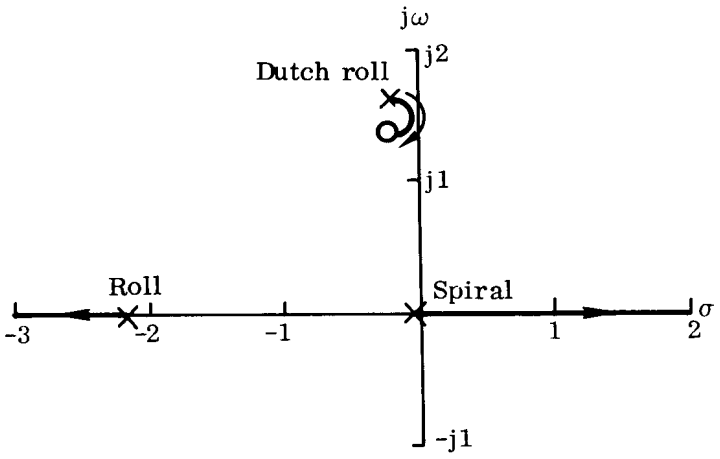

Figure 19.– Root locus for the $\frac{\delta_a}{\varphi}$ loop at 0.23L0.
(Gain values in rad/rad.)

The expression relating spiral root location will give satisfactory results as long as $\frac{1}{\tau_s}$ is not very large. It is also interesting to note that all of the aerodynamic stability derivatives augmented by previously discussed loops appear in equation (17). It is not surprising, then, that all of the feedback loops considered so far should have noticeable effects on the spiral mode.

MULTILOOP RESPONSE FEEDBACK OPERATION

The response feedback loops have thus far been considered as single-loop systems. In most practical applications, however, it is necessary for two or more loops to be used simultaneously to achieve the desired aircraft response characteristics. If, for example, it is required that both Dutch roll frequency and damping ratio be controlled, it is necessary to use more than one feedback loop, since no one loop can exercise independent control over both of these parameters. It was noted that the $\frac{\delta_r}{\beta}$ loop affects the Dutch roll frequency and the $\frac{\delta_r}{r}$ loop has its major effect on the Dutch roll

damping ratio, hence the two loops can be used together to adjust the system frequency and damping ratio. The block diagram of this system is shown in figure 20. By rearranging the diagram, it is possible to write a $\frac{\beta}{\delta_{r_p}}(s)$ transfer function for the entire closed-loop system as

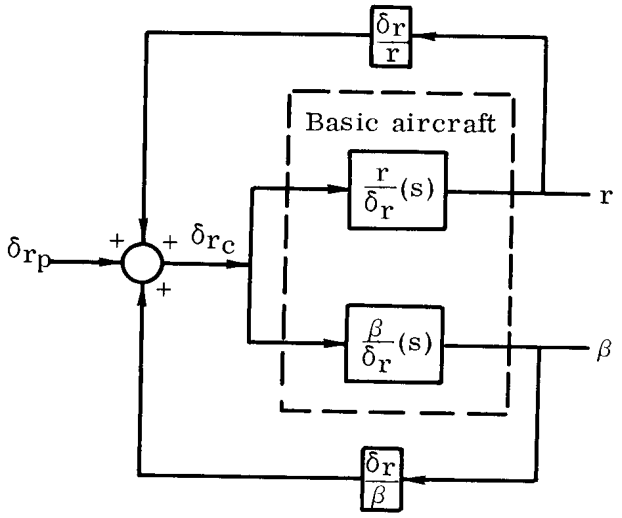

Figure 20.– Two-loop block diagram representation.

$$\frac{\beta}{\delta_{r_p}}(s) = \frac{\left[\frac{\beta}{\delta_r}(s)\right]_{basic}}{1-\left(\frac{\delta_r}{r}\right)\left[\frac{r}{\delta_r}(s)\right]_{basic}-\left(\frac{\delta_r}{\beta}\right)\left[\frac{\beta}{\delta_r}(s)\right]_{basic}} \qquad (18)$$

The characteristic equation, which is the denominator of equation (18) set equal to zero, is a function of both feedback gains, hence two variables exist which influence the movement of poles on the s-plane.

The root-locus technique can be used to analyze certain multiloop systems as shown in reference 8. The result is a root contour, as shown in figure 21. The dashed lines are constant $\frac{\delta_r}{\beta}$ gains; the solid lines represent constant values of $\frac{\delta_r}{r}$.

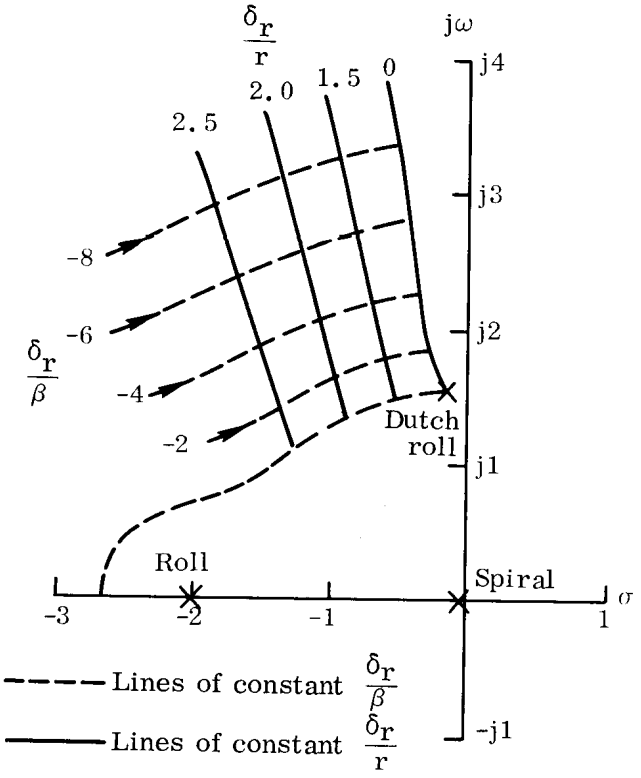

Figure 21.– Root contour for the $\frac{\delta_r}{r}$ and $\frac{\delta_r}{\beta}$ loops at 0.23L0. (Gain values for $\frac{\delta_r}{r}$ and $\frac{\delta_r}{\beta}$ in rad/rad/sec and rad/rad, respectively.)

By using such a plot, it is possible to achieve a desired ω_ψ and ζ_ψ. The roll and spiral modes are not shown in the figure, but each combination of $\frac{\delta_r}{\beta}$ and $\frac{\delta_r}{r}$ will determine a roll and a spiral time constant. If a somewhat independent means of varying τ_r is required, it will be necessary to add another loop, $\frac{\delta_a}{p}$, for example. Spiral stability may also be important; hence, a fourth loop would be necessary. Thus, there are many combinations of loops which could be used, and these configurations are dictated by the requirements on the closed-loop response.

The method for analyzing a multiloop feedback system involving a single control input, δ_{a_p} or δ_{r_p}, can be summarized as follows:

1. Close one loop and find the root locus corresponding to various values of feedback gain.

2. For one value of the feedback gain of loop number one, locate the roots (poles) and add the zeros of loop number two, disregarding the original zeros.

3. Find the root locus corresponding to the pole-zero configuration of step 2, as a function of the second feedback gain.

Note that step 3 may be repeated for every value of the first feedback gain desired, in each case using the pole locations corresponding to that gain. The resulting diagram is a root contour, showing graphically the effect of two feedback loops. The process can be expanded to more loops only if the loops have the same control-surface input. This method is not valid for a $\frac{\delta_r}{r}$ and a $\frac{\delta_a}{\beta}$ loop combination, for example, inasmuch as the implicit assumption of this technique is that closing the first loop did not alter the zeros of the second loop in figure 20. This assumption follows from the general statements made earlier concerning the effects of feedback loops on transfer-function numerators.

For multiple input-output systems, the characteristic equation must be written for the total system and factored to yield the roots which determine the transient response of the aircraft. This must be done for each combination of feedback gains. Reference 9 presents a more detailed analysis of general multiloop systems.

In some cases, it is possible to develop an expression relating two feedback gains and a dynamic mode variable. Equation (19) applies when the $\frac{\delta_r}{\beta}$ and $\frac{\delta_r}{\dot{\beta}}$ loops are used together as

$$\frac{\delta_r}{\dot{\beta}} = \frac{2\zeta_\psi\omega_\psi + N_r + Y_\beta + \left(\frac{\delta_r}{\beta}\right) Y_{\delta_r}}{N_{\delta_r} + Y_{\delta_r}\left(N_r + 2\zeta_\psi\omega_\psi\right)} \tag{19}$$

Equation (19) was obtained by examining equation (6) and noting that $\left(\frac{\delta_r}{\beta}\right) Y_{\delta_r}$ augments Y_β and indicates the required $\frac{\delta_r}{\beta}$ gain for a desired $2\zeta_\psi\omega_\psi$. The ω_ψ now is that which results from the $\frac{\delta_r}{\beta}$ loop used alone.

In most cases it is not possible to write simple expressions relating two or more feedback gains, and it is necessary to resort to factoring the total system characteristic equation, given the feedback gain values, to find the closed-loop dynamics.

ANALYSIS OF TWO-LOOP OPERATION FROM STABILITY-DERIVATIVE CONSIDERATIONS ALONE

In some cases, the use of feedback loops to alter the dynamics of an aircraft is not conveniently analyzed by root-locus methods. Although quantities such as frequency, damping, and time constants are easily picked off s-plane root-locus plots, other parameters often used in handling-qualities studies are not, such as $\frac{\omega_\varphi}{\omega_\psi}$ or $\left|\frac{\varphi}{\beta}(s)\right|_\psi$. Often, these parameters are of primary concern in a response feedback loop application. Analysis of such applications is possible by working with the equivalent aerodynamic stability derivatives, that is, the effective stability derivatives, resulting from feedback loop augmentation.

In many handling-qualities studies, it is desirable to vary the ratio $\left|\frac{\varphi}{\beta}(s)\right|_\psi$. Reference 2 contains the following simplified expression for this ratio when ζ_ψ is small:

$$\left|\frac{\varphi}{\beta}(s)\right|_\psi \simeq \left|\frac{L_\beta}{N_\beta}\right|_{\text{effective}} \tag{20}$$

Any feedback loop which augments L_β or N_β will affect the $\left|\frac{\varphi}{\beta}(s)\right|_\psi$ ratio of equation (20). Rewriting the equation to include the effects of a $\frac{\delta_r}{\beta}$ loop (where $\frac{\delta_r}{\beta}$ carries its own sign) introduces new terms as shown in the following expression:

$$\left|\frac{\varphi}{\beta}(s)\right|_\psi = \left|\frac{L_\beta + \left(\frac{\delta_r}{\beta}\right) L_{\delta_r}}{N_\beta + \left(\frac{\delta_r}{\beta}\right) N_{\delta_r}}\right| \tag{21}$$

Changes in the $\left|\frac{\varphi}{\beta}(s)\right|_\psi$ ratio are necessarily accompanied by changes in the Dutch roll natural frequency because of the N_β augmentation. The use of $\frac{\delta_a}{\beta}$ alone is likewise undesirable because of its influence on the effective N_β through the term $\left(\frac{\delta_a}{\beta}\right) N_{\delta_a}$, as shown by the following equation:

$$\left|\frac{\varphi}{\beta}(s)\right|_{\psi} = \left|\frac{L_\beta + \left(\frac{\delta_a}{\beta}\right)L_{\delta_a}}{N_\beta + \left(\frac{\delta_a}{\beta}\right)N_{\delta_a}}\right| \tag{22}$$

By using an expression for $\left|\frac{\varphi}{\beta}(s)\right|_{\psi}$ which includes the effect of both the $\frac{\delta_r}{\beta}$ and the $\frac{\delta_a}{\beta}$ loops, it is possible to obtain a desired $\left|\frac{\varphi}{\beta}(s)\right|_{\psi}$ ratio and yet maintain the effective N_β constant, assuming that N_β is an accurate approximation to $\omega_\psi{}^2$, that is, the $\alpha_T L_\beta$ is small due to a small α_T. This expression is

$$\left|\frac{\varphi}{\beta}(s)\right|_{\psi} = \left|\frac{L_\beta + \left(\frac{\delta_r}{\beta}\right)L_{\delta_r} + \left(\frac{\delta_a}{\beta}\right)L_{\delta_a}}{N_\beta + \left(\frac{\delta_r}{\beta}\right)N_{\delta_r} + \left(\frac{\delta_a}{\beta}\right)N_{\delta_a}}\right| \tag{23}$$

If the total effective N_β is to remain constant at the open-loop value, the relation

$$\frac{\delta_r}{\beta} = -\left(\frac{\delta_a}{\beta}\right)\frac{N_{\delta_a}}{N_{\delta_r}} \tag{24}$$

must be satisfied. Substituting equation (24) into equation (23) results in the expression

$$\left|\frac{\varphi}{\beta}(s)\right|_{\psi} = \left|\frac{L_\beta + \frac{\delta_a}{\beta}\left(L_{\delta_a} - \frac{N_{\delta_a}L_{\delta_r}}{N_{\delta_r}}\right)}{N_\beta}\right| \tag{25}$$

The desired $\left|\frac{\varphi}{\beta}(s)\right|_{\psi}$ ratio can be obtained by solving for the $\frac{\delta_a}{\beta}$ gain in equation (25), then solving for the corresponding $\frac{\delta_r}{\beta}$ gain from equation (24). The absolute-value sign indicates that there will be two sets of gains which will satisfy equation (25). The selection of the sign of the $\frac{\delta_a}{\beta}$ gain to be used must be made in the light of other considerations, such as the fact that L_β is an important handling-qualities parameter in itself, and for conventional aircraft in the transport category has a minus sign associated with it, which indicates positive dihedral. This means that the sign of the $\frac{\delta_a}{\beta}$ gain must be chosen that will maintain the total effective L_β as a negative quantity.

Other dynamic side effects of the two-loop combination used here, such as the influence on the spiral mode, may dictate the use of other loops to maintain a flyable vehicle. The effect of these other loops on the $\left|\frac{\varphi}{\beta}(s)\right|_{\psi}$ ratio, in turn, may have to be taken into account. Iterative processes will usually be necessary to determine the final

combination of gains, and these processes are best handled by a digital computer. For some cases when equation (20) is valid, equation (25) may be adequate to calculate the required gains. In the preceding example, it was assumed that it was necessary to hold N_β constant at the open-loop value, but equation (24) could just have easily been written to attain some other desired effective N_β. In practice, there will be many cases in which equation (20) will not be adequate. This must be determined first. The simplified approximation to $\left|\frac{\varphi}{\beta}(s)\right|_\psi$ was used to illustrate the equivalent stability-derivative approach in a two-loop situation.

EFFECT OF ACTUATOR DYNAMICS ON RFS PERFORMANCE

Analysis of the response feedback loops has been carried out on an idealized system where neither sensors nor actuators display any phase lag. The scope of this paper does not warrant a detailed examination of all the associated effects of sensor and servo dynamics; however, it is worthwhile at this point to consider how these effects can be included in the analysis of a typical feedback loop.

The problem of phase lags in a response feedback system is a serious one. Generally, sensors, such as gyros, accelerometers, and vanes, can be expected to have less phase lag than the actuators at operating frequencies. The effect of actuator dynamics on response-feedback-system performance is, then, of primary interest.

A suitable mathematical model must be chosen to represent the actuator. One such model is shown in figure 22. The actuator can be shown in the aircraft response feedback system in the forward loop as in figure 23. The closed-loop transfer function can then be written as

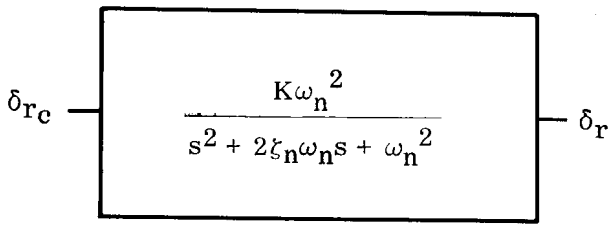

Figure 22.– Mathematical model of a second-order actuator.

$$\frac{\beta}{\delta_{r_p}}(s) = \frac{\left[\frac{\delta_r}{\delta_{r_c}}(s)\right]\left[\frac{\beta}{\delta_r}(s)\right]_{basic}}{1 - \left(\frac{\delta_r}{\beta}\right)\left[\frac{\delta_r}{\delta_{r_c}}(s)\right]\left[\frac{\beta}{\delta_r}(s)\right]_{basic}} \qquad (26)$$

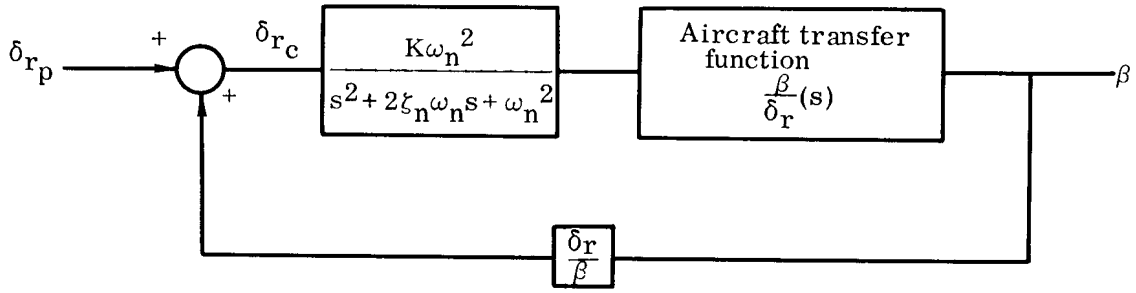

Figure 23.– Inclusion of actuator in RFS loop.

The order of the characteristic equation is increased from a fourth- to a sixth-order equation. The phase lag of the actuator itself can be calculated at any driving frequency ω as

$$\varphi_A = \tan^{-1} \frac{2\zeta_n\left(\frac{\omega}{\omega_n}\right)}{1 - \left(\frac{\omega}{\omega_n}\right)^2} \tag{27}$$

It is apparent from equation (27) that in order to minimize phase lag ω_n should be as large as possible for a given ζ_n.

The addition of an actuator in the forward loop does not greatly increase the labor required for analysis by the root-locus method. The poles (and zeros, if any) of the actuator transfer function are placed on the s-plane with the poles and zeros of the $\frac{\beta}{\delta_r}(s)$ transfer function. The location of the actuator poles is a function of ζ_n and ω_n. It is usually desirable to have approximately 70 percent critical damping for the actuators. The effect of such a 70-percent damped actuator on the $\frac{\delta_r}{\beta}$ loop and its influence on the Dutch roll are shown in figure 24.

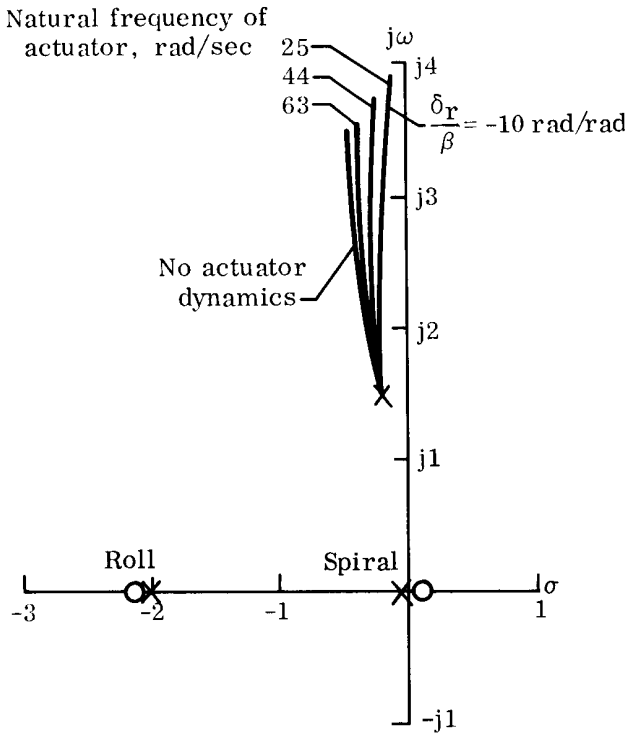

Figure 24.– Effect of actuator on Dutch roll dynamics with the $-\frac{\delta_r}{\beta}$ loop closed at 0.23L0.

The locus for the system when actuator dynamics are neglected was discussed in the section on the $\frac{\delta_r}{\beta}$ loop. The 63 rad/sec actuator has destabilized the Dutch roll by decreasing the damping ratio. For an actuator with a natural frequency of 25 rad/sec, the Dutch roll can be made to go divergent if the gain is high enough, in this case, above 20 rad/rad. Actuators with natural frequencies less than 25 rad/sec would cause instability at lower values of feedback gain.

The roll and spiral modes will not be affected noticeably unless they form a lateral phugoid and break away from the real axis. The breakaway point itself will be dependent somewhat on actuator pole location. The representation of the actuator may be different from the ideal second-order type assumed here. Position rate or pressure rate feedbacks around the actuator, along with other compensation, could result in a higher

order representation with possible numerator roots. In this case, the roll and spiral modes would be influenced. It is also important that the actuator poles be examined as the feedback gain is increased. While it is possible that these poles will move into the right-half plane, resulting in an unstable system, it is also likely that they may move toward the real axis, indicating that the damping ratio of the actuator is increasing. Equation (27) shows that the phase lag will increase with increasing ζ_n, and it is undesirable to add any more phase lag to the system.

The importance of including actuator dynamics in practical applications is evident from figure 24, and especially when high gain feedback loops are used with low frequency actuators.

CONCLUSIONS

On the basis of an analysis of the response feedback system for the lateral-directional modes of a variable-stability transport airplane, the following general conclusions can be drawn:

1. Each feedback loop influences all of the aircraft dynamic modes but, in most cases, displays one dominant effect.

2. For values of feedback gain that are considered to be reasonable for this airplane, most classical approximations of loop action were valid.

3. The analytically derived gain expressions have conditions of validity associated with them, and it is important to ascertain that these conditions are satisfied.

4. The equivalent stability-derivative method of analysis is valuable when root-locus diagrams are not convenient to show loop effects.

5. Root-locus analysis techniques can be expanded to miltiloop configurations, but it must be realized that the methods outlined herein are applicable only to loop combinations that do not alter the numerators of transfer functions in the closed loop.

6. Actuator dynamics can be readily included in a root-locus analysis. In more detailed studies of response feedback systems it will usually be necessary to include actuator effects.

7. Practical limitations will determine the final success of a response feedback system. These limitations must be included in the analysis as demanded by the particular application.

Flight Research Center,
National Aeronautics and Space Administration,
Edwards, Calif., December 14, 1966
720-04-00-01-24

APPENDIX A

EQUATIONS OF MOTION USED IN LATERAL-DIRECTIONAL RFS STUDY

The side-force and moment equations (ref. 11) are written in a set of orthogonal body-axis coordinates. The three equations written in conventional nonlinear form are as follows:

Side force -

$$m(\dot{v} + ru - pw) = mg \sin \varphi \cos \Theta + \frac{1}{2}\rho V^2 S(-C_D \sin \beta + C_Y \cos \beta)$$

Rolling moment -

$$\dot{p}I_{XX} - \dot{r}I_{XZ} + (I_{ZZ} - I_{YY})\, qr - pqI_{XZ} = \frac{1}{2}\rho V^2 SbC_l$$

Yawing moment -

$$\dot{r}I_{ZZ} - \dot{p}I_{XZ} + (I_{YY} - I_{XX})\, pq + qrI_{XZ} = \frac{1}{2}\rho V^2 SbC_n$$

These three equations are modified by assuming that, in still air,

$$\alpha \approx \frac{w}{V}$$

$$\beta \approx \frac{v}{V}$$

$$\dot{\beta} \approx \frac{\dot{v}}{V} - \beta\frac{\dot{V}}{V}$$

To further reduce complexity with little loss in accuracy, the following approximations are made:

1. Inertia coupling terms in the moment equations are dropped
2. $\dot{\beta} \approx \frac{\dot{v}}{V}$
3. $-C_D \sin \beta + C_Y \cos \beta$ is approximated by C_Y

4. V is used for u in the side-force equation

The side-force equation then becomes

$$m(\dot{v} + rV - pw) = mg \sin \varphi \cos \Theta + \frac{1}{2}\rho V^2 S C_Y$$

Dividing by mV,

$$\frac{\dot{v}}{V} + r - p\frac{w}{V} = \frac{g}{V} \sin \varphi \cos \Theta + \frac{\rho VS}{2m} C_Y$$

Incorporating the approximations,

$$\dot{\beta} = \frac{\rho VS}{2m} C_Y + \frac{g}{V} \sin \varphi \cos \Theta + p\alpha - r$$

The rolling-moment equation is

$$\dot{p} = \frac{1}{I_{XX}}(\dot{r} I_{XZ} + \frac{1}{2}\rho V^2 Sb C_l)$$

The yawing-moment equation is

$$\dot{r} = \frac{1}{I_{ZZ}}(\dot{p} I_{XZ} + \frac{1}{2}\rho V^2 Sb C_n)$$

The three equations are then linearized about a trim flight condition ($V = V_T$) where the initial p, r, φ, ψ, β, δ_r, and δ_a are zero. The resultant linearized perturbation equations are (assuming $C_{Y_{\dot{\beta}}} = C_{Y_{\delta_a}} = C_{l_{\dot{\beta}}} = 0$)

Side force -

$$\dot{\beta} = \rho \frac{V_T S}{2m} \left(C_{Y_\beta} \beta + C_{Y_{\delta_r}} \delta_r\right) + \rho \frac{V_T S}{2m} \left(\frac{b}{2V_T}\right) C_{Y_r} r + \frac{g}{V_T} \varphi + p\alpha_T - r$$

Rolling moment -

$$\dot{p} = \frac{I_{XZ}}{I_{XX}} \dot{r} + \frac{1}{I_{XX}} \left[\frac{1}{2} \rho V_T^2 Sb \left(C_{l_\beta} \beta + C_{l_{\delta_r}} \delta_r + C_{l_{\delta_a}} \delta_a\right) + \frac{1}{2} \rho V_T^2 Sb \left(\frac{b}{2V_T}\right) \left(C_{l_r} r + C_{l_p} p\right)\right]$$

Yawing moment -

$$\dot{r} = \frac{I_{XZ}}{I_{ZZ}}\dot{p} + \frac{1}{I_{ZZ}}\left[\frac{1}{2}\rho V_T{}^2 Sb\left(C_{n_\beta}\beta + C_{n_{\delta_r}}\delta_r + C_{n_{\delta_a}}\delta_a\right) + \frac{1}{2}\rho V_T{}^2 Sb\left(\frac{b}{2V_T}\right)\left(C_{n_r}r + C_{n_p}p\right)\right]$$

As a further modification to conserve analog equipment necessary for programing, the Euler angular rate relationship is solved for p as

$$p = \dot{\varphi} - \dot{\psi}\sin\Theta$$

Substituting the Euler expression for $\dot{\psi}$,

$$p = \dot{\varphi} - (q\sin\varphi + r\cos\varphi)\tan\Theta$$

Linearizing this expression and assuming $\tan\Theta_T = \tan\alpha_T = \alpha_T$,

$$p = \dot{\varphi} - r\alpha_T$$

Differentiating,

$$\dot{p} = \ddot{\varphi} - \dot{r}\alpha_T$$

Substituting p and $\dot{p}$ into the three equations and rearranging, using the dimensional forms of the aerodynamic stability derivatives, yields the final form of the lateral-directional equations of motion. Note that the equations are now in terms of an earth reference, $\dot{\varphi}$ and $\ddot{\varphi}$, rather than a body axis, p and $\dot{p}$, as follows:

Side force -

$$(1 - Y_r + \alpha_T{}^2)r + \dot{\beta} - Y_\beta\beta - \alpha_T\dot{\varphi} - \frac{g}{V_T}\varphi = Y_{\delta_r}\delta_r$$

Rolling moment -

$$-\left(\alpha_T + \frac{I_{XZ}}{I_{XX}}\right)\dot{r} + (\alpha_T L_p - L_r)r - L_\beta\beta + \ddot{\varphi} - L_p\dot{\varphi} = L_{\delta_a}\delta_a + L_{\delta_r}\delta_r$$

Yawing moment -

$$\left(1 + \alpha_T\frac{I_{XZ}}{I_{ZZ}}\right)\dot{r} + (\alpha_T N_p - N_r)r - N_\beta\beta - \frac{I_{XZ}}{I_{ZZ}}\ddot{\varphi} - N_p\dot{\varphi} = N_{\delta_a}\delta_a + N_{\delta_r}\delta_r$$

APPENDIX A

By Laplace transforming the equations and using the variable s, the equations can be written as

Side force -

$$(1 - Y_r + \alpha_T{}^2)\, r + (s - Y_\beta)\beta - \left(\alpha_T s + \frac{g}{V_T}\right) \varphi = Y_{\delta_r}\delta_r$$

Rolling moment -

$$\left[-\left(\alpha_T + \frac{I_{XZ}}{I_{XX}}\right) s + (\alpha_T L_p - L_r)\right] r - L_\beta \beta + (s^2 - L_p s)\, \varphi = L_{\delta_a}\delta_a + L_{\delta_r}\delta_r$$

Yawing moment -

$$\left[\left(1 + \alpha_T \frac{I_{XZ}}{I_{ZZ}}\right) s + (\alpha_T N_p - N_r)\right] r - N_\beta \beta - \left(\frac{I_{XZ}}{I_{ZZ}}\, s^2 + N_p s\right) \varphi = N_{\delta_a}\delta_a + N_{\delta_r}\delta_r$$

APPENDIX B

APPLICATION OF ROOT-LOCUS METHODS TO ANALYSIS OF RESPONSE FEEDBACK LOOPS

The root-locus method of analysis (refs. 7 and 8) directly relates feedback gain values and characteristic equation roots. It is these roots that determine the form of the response of the dynamic system. Generally, the characteristic equation for the lateral-directional mode is a fourth-order equation which, for the transport class of aircraft, usually factors into the following form (ref. 5):

$$(s^2 + 2\zeta_\psi \omega_\psi s + \omega_\psi{}^2)\left(s + \frac{1}{\tau_r}\right)\left(s + \frac{1}{\tau_s}\right) = 0$$

Each parenthetical term is referred to as a dynamic mode. The second-order term is the Dutch roll mode, and the two first-order terms are the roll and spiral modes, respectively. Adequate descriptions of the physical characteristics of these modes are found in most texts on aircraft dynamics. For the analyses of this paper it is sufficient to note that each parenthetical term in the equation in the Laplace variable (frequency domain) has an equivalent form in the time domain, as explained in references 7 and 8. The Dutch roll is an exponentially varying sinusoidal oscillation of the general form

$$e^{-\zeta_\psi \omega_\psi t} \sin(\omega t + \lambda)$$

where λ is an arbitrary phase angle. The roll and spiral modes are, respectively, exponential functions of the form $e^{-\frac{t}{\tau_r}}$ and $e^{-\frac{t}{\tau_s}}$. The root-locus technique provides a convenient method of plotting the roots of the characteristic equation as a function of the particular feedback gain used. The resultant curve, presented on the s-plane, yields information about the dynamic stability of each of the modes. Figure 25 shows the three modes and indicates the parameters characteristic of the dynamics of each mode.

The basic aircraft characteristic equation roots are designated by X's and are referred to as poles. The Dutch roll mode appears as two poles because the roots of the second-order term in the characteristic equation are a complex pair. The magnitude of the distance between the origin and one Dutch roll pole is the undamped natural frequency in radians/second. The component of this distance along the imaginary axis is the damped frequency that would be measured on a time history. The damping ratio of the Dutch roll is the cosine of the angle between the negative real axis and a line drawn from the origin to the pole. The roll and spiral mode time constants, in seconds, correspond to the inverse of the distance between the origin and the pole location. If a root lies to the left of the $j\omega$ axis, the resultant time response is stable; whereas, roots falling to the right of the $j\omega$ axis are unstable. Roots falling on the $j\omega$ axis are termed neutrally stable.

APPENDIX B

Graphical techniques used in plotting root-locus diagrams utilize the transfer function numerator roots (zeros) as well as the poles. These zero locations are designated by ○'s and are shown herein on root-locus diagrams. The graphical techniques are described in references 7 and 8.

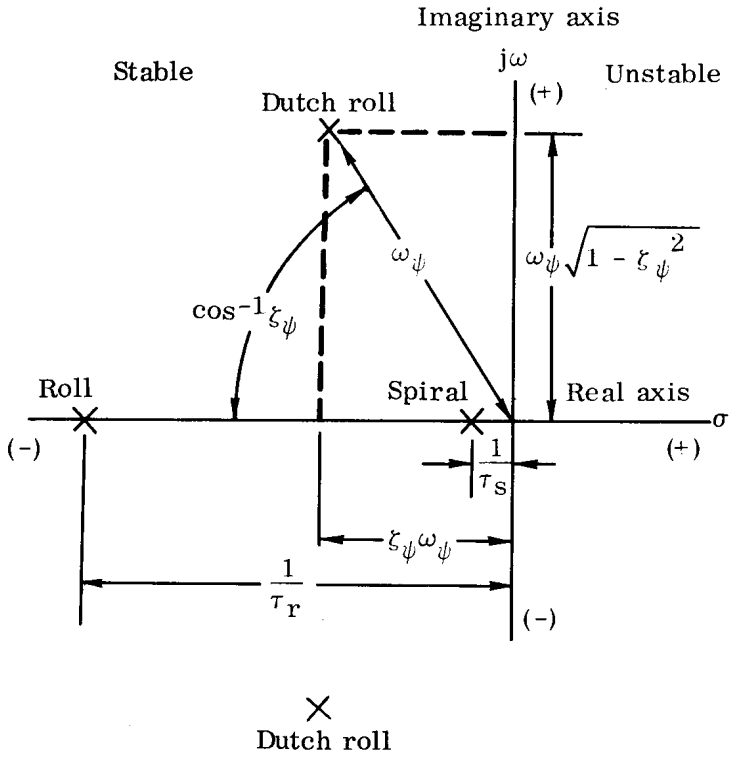

Figure 25.– Lateral-directional modes as displayed on the complex or s-plane.

APPENDIX C

TWO-DEGREE-OF-FREEDOM APPROXIMATION TO THE DUTCH ROLL WITH THE $\frac{\delta_r}{r}$ LOOP

By choosing only the dominant terms in the equation of motion, the side-force and yawing-moment equations become

$$(s - Y_\beta)\beta + r = Y_{\delta_r}\delta_r$$

and

$$-N_\beta\beta + (s - N_r)r = N_{\delta_r}\delta_r$$

allowing only β and r motions. Now letting $\delta_r = \delta_{r_p} + \left(\frac{\delta_r}{r}\right)r$,

$$(s - Y_\beta)\beta + r = Y_{\delta_r}\delta_{r_p} + \left(\frac{\delta_r}{r}\right)Y_{\delta_r}r$$

$$-N_\beta\beta + (s - N_r)r = N_{\delta_r}\delta_{r_p} + \left(\frac{\delta_r}{r}\right)N_{\delta_r}r$$

or

$$(s - Y_\beta)\beta + \left[1 - \left(\frac{\delta_r}{r}\right)Y_{\delta_r}\right]r = Y_{\delta_r}\delta_{r_p}$$

$$-N_\beta\beta + \left[s - N_r - \left(\frac{\delta_r}{r}\right)N_{\delta_r}\right]r = N_{\delta_r}\delta_{r_p}$$

the characteristic equation is

$$s^2 - \left[N_r + Y_\beta + \left(\frac{\delta_r}{r}\right)N_{\delta_r}\right]s + N_\beta + N_rY_\beta + \left(\frac{\delta_r}{r}\right)\left(N_{\delta_r}Y_\beta - N_\beta Y_{\delta_r}\right) = 0$$

In similar fashion, writing $\delta_r = \delta_{r_p} + \left(\frac{\delta_r}{\beta}\right)\beta$, the two-degree-of-freedom approximation to the Dutch roll can be used to obtain the characteristic equation

$$s^2 - \left[N_r + Y_\beta + \left(\frac{\delta_r}{\beta}\right)Y_{\delta_r}\right]s + N_\beta + N_rY_\beta + \frac{\delta_r}{\beta}\left(N_{\delta_r} + N_rY_{\delta_r}\right) = 0$$

APPENDIX D

ANALYTICAL EXPRESSION RELATING $\frac{\delta_r}{\dot{\beta}}$ TO $2\zeta_\psi\omega_\psi$ OF THE DUTCH ROLL

The expanded characteristic equation general literal form is easily shown (ref. 5) to be

$$s^4 + \left(2\zeta_\psi\omega_\psi + \frac{1}{\tau_r} + \frac{1}{\tau_s}\right)s^3$$

$$+\left(\omega_\psi{}^2 + \frac{2\zeta_\psi\omega_\psi}{\tau_r} + \frac{2\zeta_\psi\omega_\psi}{\tau_s} + \frac{1}{\tau_r\tau_s}\right)s^2$$

$$+\left(\frac{\omega_\psi{}^2}{\tau_r} + \frac{\omega_\psi{}^2}{\tau_s} + \frac{2\zeta_\psi\omega_\psi}{\tau_r\tau_s}\right)s$$

$$+\left(\frac{\omega_\psi{}^2}{\tau_r\tau_s}\right) = 0$$

Comparing the coefficients of this equation with

$$s^4 + \frac{B}{A}s^3 + \frac{C}{A}s^2 + \frac{D}{A}s + \frac{E}{A} = 0$$

which is the general form of a fourth-order algebraic equation where the coefficient of the highest order term s^4 has been made equal to unity, and equating the s^3 terms of the two equations results in

$$\frac{B}{A} = 2\zeta_\psi\omega_\psi + \frac{1}{\tau_r} + \frac{1}{\tau_s}$$

For most transport aircraft, $\frac{1}{\tau_s}$ can be neglected with respect to the other two terms. Also, to a very good approximation

$$\frac{1}{\tau_r} = -L_p$$

and so

$$\frac{B}{A} = 2\zeta_\psi\omega_\psi - L_p$$

APPENDIX D

After writing the feedback loop equation as

$$\delta_r = \delta_{r_p} + \left(\frac{\delta_r}{\dot{\beta}}\right)\dot{\beta}$$

and substituting into the lateral-directional equations of motion, the characteristic equation can be found. The coefficient of s^4 term (A) is

$$\left[1 - \left(\frac{\delta_r}{\dot{\beta}}\right) Y_{\delta_r}\right]\left[\left(1 + \alpha_T \frac{I_{XZ}}{I_{ZZ}}\right) - \frac{I_{XZ}}{I_{ZZ}}\left(\alpha_T + \frac{I_{XZ}}{I_{XX}}\right)\right]$$

and the coefficient of s^3 term (B) is

$$\left[1 - \left(\frac{\delta_r}{\dot{\beta}}\right) Y_{\delta_r}\right]\left[(\alpha_T N_p - N_r) + \frac{I_{XZ}}{I_{ZZ}}(\alpha_T L_p - L_r)\right]$$

$$-\left(1 + \alpha_T \frac{I_{XZ}}{I_{ZZ}}\right)\left[L_p + Y_\beta + \left(\frac{\delta_r}{\dot{\beta}}\right)\left(\alpha_T L_{\delta_r} - L_p Y_{\delta_r}\right)\right]$$

$$-\left(\alpha_T + \frac{I_{XZ}}{I_{XX}}\right)\left[N_p - Y_\beta \frac{I_{XZ}}{I_{ZZ}} + \left(\frac{\delta_r}{\dot{\beta}}\right)\left(\alpha_T N_{\delta_r} - N_p Y_{\delta_r}\right)\right]$$

$$+\left(1 - Y_r + \alpha_T{}^2\right)\left(\frac{\delta_r}{\dot{\beta}}\right)\left(N_{\delta_r} + L_{\delta_r}\frac{I_{XZ}}{I_{ZZ}}\right)$$

The s^4 and s^3 coefficients can be simplified by neglecting small triple-product terms; inertia terms, since $\frac{I_{XZ}}{I_{XX}}$ and $\frac{I_{XZ}}{I_{ZZ}}$, small numbers themselves, appear in products usually much smaller than other terms in the sum; and terms involving α_T, since the trim angle of attack is assumed to be small. Using the remaining significant terms, the first two terms of the characteristic equation are

$$s^4\left[1 - \left(\frac{\delta_r}{\dot{\beta}}\right) Y_{\delta_r}\right]$$

and

$$s^3\left[-L_p - N_r - Y_\beta + \left(\frac{\delta_r}{\dot{\beta}}\right)\left(L_p Y_{\delta_r} + N_r Y_{\delta_r} + N_{\delta_r}\right)\right]$$

But, as shown previously,

$$\frac{B}{A} = 2\zeta_\psi \omega_\psi - L_p$$

and, substituting the expressions derived for A and B,

$$\frac{B}{A} = \frac{-L_p - N_r - Y_\beta + \left(\frac{\delta_r}{\dot{\beta}}\right)\left(L_p Y_{\delta_r} + N_r Y_{\delta_r} + N_{\delta_r}\right)}{1 - \left(\frac{\delta_r}{\dot{\beta}}\right) Y_{\delta_r}}$$

Equating the two expressions for $\frac{B}{A}$ and solving for $\frac{\delta_r}{\dot{\beta}}$,

$$\frac{\delta_r}{\dot{\beta}} \simeq \frac{2\zeta_\psi \omega_\psi + N_r + Y_\beta}{N_{\delta_r} + Y_{\delta_r}\left(N_r + 2\zeta_\psi \omega_\psi\right)}$$

APPENDIX E

APPROXIMATION TO THE SPIRAL MODE TIME CONSTANT WHEN $\frac{\delta_a}{\varphi}$ IS USED AS A FEEDBACK LOOP

Reference 5 states that if the spiral mode constant τ_s is very large,

$$\frac{1}{\tau_s} \simeq \frac{E}{D}$$

where D and E are the coefficients of the s^1 and s^0 terms, respectively, of the lateral-directional characteristic equation. If the auxiliary feedback equation is written as

$$\delta_a = \delta_{a_p} + \left(\frac{\delta_a}{\varphi}\right)\varphi$$

D, the coefficient of the s^1 term, is

$$D = -(\alpha_T N_p - N_r)\left[\alpha_T L_\beta - L_p Y_\beta + \left(\frac{\delta_a}{\varphi}\right) L_{\delta_a}\right]$$

$$+(\alpha_T L_p - L_r)\left[\alpha_T N_\beta - N_p Y_\beta + \left(\frac{\delta_a}{\varphi}\right) N_{\delta_a}\right]$$

$$-(1 - Y_r + \alpha_T{}^2)(L_p N_\beta - L_\beta N_p)$$

$$-\left(\alpha_T + \frac{I_{XZ}}{I_{XX}}\right)\left[\frac{g}{V_T} N_\beta - \left(\frac{\delta_a}{\varphi}\right) N_{\delta_a} Y_\beta\right]$$

$$-\left(1 + \alpha_T \frac{I_{XZ}}{I_{ZZ}}\right)\left[\frac{g}{V_T} L_\beta - \left(\frac{\delta_a}{\varphi}\right) L_{\delta_a} Y_\beta\right]$$

The E term is

$$E = -(\alpha_T N_p - N_r)\left[\frac{g}{V_T} L_\beta - \left(\frac{\delta_a}{\varphi}\right) L_{\delta_a} Y_\beta\right]$$

$$+(\alpha_T L_p - L_r)\left[\frac{g}{V_T} N_\beta - \left(\frac{\delta_a}{\varphi}\right) N_{\delta_a} Y_\beta\right]$$

$$-(1 - Y_r + \alpha_T{}^2)\left[\left(\frac{\delta_a}{\varphi}\right) L_{\delta_a} N_\beta - \left(\frac{\delta_a}{\varphi}\right) L_\beta N_{\delta_a}\right]$$

Neglecting small triple-product terms and assuming that inertia terms are small, since $\frac{I_{XZ}}{I_{ZZ}} << 1$ for the JetStar,

$$D = L_\beta N_p - L_p N_\beta - \frac{g}{V_T} L_\beta + \left(\frac{\delta_a}{\varphi}\right)\left[L_{\delta_a}(N_r + Y_\beta) + N_{\delta_a}\left(\alpha_T Y_\beta - L_r\right)\right]$$

For the JetStar,

$$L_{\delta_a}(N_r + Y_\beta) \gg N_{\delta_a}\left(\alpha_T Y_\beta - L_r\right)$$

and

$$D = L_\beta N_p - L_p N_\beta - \frac{g}{V_T} L_\beta + \left(\frac{\delta_a}{\varphi}\right)\left[L_{\delta_a}\left(N_r + Y_\beta\right)\right]$$

Similarly for the E term, neglecting small triple-product terms and inertia terms,

$$E = \frac{g}{V_T}\left(L_\beta N_r - L_r N_\beta\right) - \left(\frac{\delta_a}{\varphi}\right)\left[L_{\delta_a}\left(N_r Y_\beta + N_\beta\right) - N_{\delta_a}\left(L_r Y_\beta + L_\beta\right)\right]$$

For the JetStar,

$$N_\beta \gg N_r Y_\beta$$

$$L_\beta \gg L_r Y_\beta$$

$$E = \frac{g}{V_T}\left(L_\beta N_r - L_r N_\beta\right) - \left(\frac{\delta_a}{\varphi}\right)\left(L_{\delta_a} N_\beta - L_\beta N_{\delta_a}\right)$$

Furthermore, for most cases,

$$L_{\delta_a} N_\beta \gg L_\beta N_{\delta_a}$$

and so the fraction $\frac{E}{D}$ can be written as

$$\frac{E}{D} \simeq \frac{1}{\tau_s} \simeq \frac{\frac{g}{V_T}\left(L_\beta N_r - L_r N_\beta\right) - \left(\frac{\delta_a}{\varphi}\right) L_{\delta_a} N_\beta}{L_\beta N_p - L_p N_\beta - \frac{g}{V_T} L_\beta + \left(\frac{\delta_a}{\varphi}\right)\left[L_{\delta_a}\left(N_r + Y_\beta\right)\right]}$$

REFERENCES

1. Ball, J. N.; et al.: Installation of an Automatic Control System in a T-33 Airplane for Variable Stability Flight Research. Part 1 - Preliminary Investigation and Design Studies. Tech. Rep. 55-156 (Cornell Rep. No. TB-936-F-1), Wright Air Dev. Center, U.S. Air Force, Apr. 1955.

2. Kidd, Edwin A.; and Harper, Robert P., Jr.: Fixed-Base and In-Flight Simulations of Longitudinal and Lateral-Directional Handling Qualities for Piloted Reentry Vehicles. Tech. Doc. Rep. No. ASD-TDR-61-362, Air Force Systems Command, Wright-Patterson Air Force Base, Feb. 1964.

3. Kidd, Edwin A.; Bull, Gifford; and Harper, Robert P., Jr.: In-Flight Simulation — Theory and Application. Rep. No. 368, AGARD, 1961.

4. Anon.: Flight Evaluations of the Effect of Variable Spiral Damping in a JTB-26B Airplane. Rep. No. TB-1094-F-1, Cornell Aero. Lab., Inc., Oct. 19, 1957.

5. Ashkenas, Irving L.; and McRuer, Duane T.: Approximate Airframe Transfer Functions and Application to Single Sensor Control Systems. Tech. Rep. 58-82 (ASTIA No. AD 151025), Wright Air Dev. Center, U.S. Air Force, June 1958.

6. Mechtly, E. A.: The International System of Units - Physical Constants and Conversion Factors. NASA SP-7012, 1964.

7. Evans, Walter R.: Control-System Dynamics. McGraw-Hill Book Co., Inc., 1954.

8. Kuo, Benjamin C.: Automatic Control Systems. Prentice-Hall, Inc., 1962.

9. McRuer, D. T.; Ashkenas, I. L.; and Pass, H. R.: Analysis of Multiloop Vehicular Control Systems. Tech. Doc. Rep. No. ASD-TDR-62-1014, Air Force Systems Command, Wright-Patterson Air Force Base, Mar. 1964.

10. Anderson, Seth B.; Quigley, Hervey C.; and Innis, Robert C.: Stability and Control Considerations for STOL Aircraft. Rep. No. 504, AGARD, 1965.

11. Clark, Daniel C.; and Kroll, John: General Purpose Airborne Simulator - Conceptual Design Report. NASA CR-544, 1966.